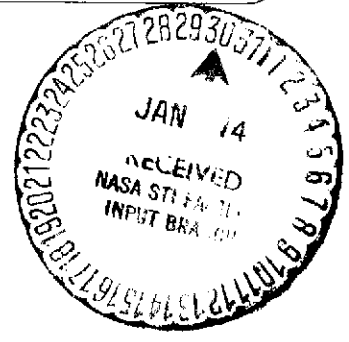


2mip

NASA CR-132898



(NASA-CR-132898) FEASIBILITY MODEL OF A HIGH RELIABILITY FIVE-YEAR TAPE TRANSPORT, VOLUME 2 Technical Report, 5 Jan. 1972 - 5 Nov. 1973 (IIT Research Inst.) 93 p HC \$6.75	N74-14895
CSSL 05B G3/07	Unclas 27002



FEASIBILITY MODEL OF A HIGH  
RELIABILITY FIVE-YEAR TAPE TRANSPORT

Technical Report - Volume II

IITRI Project No. E6225

Contract No. NAS5-21692

Goddard Space Flight Center  
Greenbelt, Maryland

TECHNICAL REPORT - VOLUME II

FEASIBILITY MODEL OF A HIGH  
RELIABILITY FIVE-YEAR TAPE TRANSPORT

(5 January 1972 - 5 November 1973)

Contract No. NAS5-21692

Prepared by:

R. L. Eshleman  
A. P. Meyers  
W. A. Davidson  
R. C. Gortowski  
M. E. Anderson

Submitted by:

IIT Research Institute  
10 West 35th Street  
Chicago, Illinois 60616

For:

Goddard Space Flight Center  
Greenbelt, Maryland

October 1973

IIT RESEARCH INSTITUTE

## FOREWORD

This is the final report on IIT Research Institute Project No. E6225 entitled: "Feasibility Model of a High Reliability Five-Year Tape Transport." The work was performed for the National Aeronautics and Space Administration, Goddard Space Flight Center under Contract No. NAS5-21692. The work was completed over a 21 month period and was monitored by Mr. Carl Powell of GSFC.

The project was divided into two major phases, the first being the design, development and fabrication of the High Reliability Five-Year Tape Transport, and the second being the analytical and experimental evaluation of its performance and reliability.

Results of this program are reported in three separate volumes. These include, Volume I - Summary Report, which provides an overview of the transport development, its performance and test results, and sets forth the conclusions and recommendations. Volume II contains a description of the system design, the analyses performed, and results of the tests performed to determine the transport's performance capability. The third volume contains all appendices and presents the detailed drawings and analytical tools used in the various analyses.

Respectfully submitted,

IIT RESEARCH INSTITUTE



M. E. Anderson  
Assistant Director of Research  
Electronics Division

Approved by:

  
Sidney Bass, Director of Research

IIT RESEARCH INSTITUTE

## ABSTRACT

The main objective of this program was the design and fabrication of a spacecraft tape recorder possessing high reliability and long life. Design of the five Year High Reliability Tape Recorder was based on the design criteria established during NASA GSFC Contract NAS5-21556, entitled; "Design Study for a High Reliability 5 Year Spacecraft Tape Transport". The design criteria established allowable dimensions for capstans, rollers, guides, heads, etc., which would not overstress the tape in its transfer from one storage reel to the other.

Based on experience gained in a study of a number of spacecraft tape transports, a philosophy for the design was established. This involved the minimization of gears, belts, pulleys and mechanical elements which have been known to cause premature failure. The resulting system design is a transport in which no mechanical couplings are used. Rather, four drive motors, one for each reel and one for each of the two capstans are used in a differential mode. There are two other modular designed tape guidance rollers which are hybrid, spherical, cone tapered-crown rollers for tape guidance. The two capstan approach provides capability of isolating the tape tension required for guidance and tape storage from that which is necessary for assuring intimate head-to-tape contact without excessive wear.

The performance objectives to which this 5-Year High Reliability Tape Transport was designed were selected on the basis of requirements for use in a specific space application calling for 100 minutes of 1.2 megabits per second recording capacity, thus representing a total capacity of  $7.2 \times 10^9$  bits. Also, a requirement for a record:playback speed ratio of 24:1 was established. Electronic control circuitry was designed and fabricated for use during the test and evaluation effort, including both tension and torque type control for the movement of tape between reels.

Analysis of the design features of the modularized tape transport renders a life expectancy in excess of five years. Tests performed on the 5 Year High Reliability Tape Transport were directed toward determining its performance capability. These tests revealed that the tape jitter and skew are in the range achieved by high quality digital tape transports. Guidance of the tape in the lateral sense by the use of the two hybrid crowned rollers proved to be excellent. Tracking was maintained within less than one thousandth inch (approximately 2 micrometers).

The guidance capability demonstrated makes possible the achievement of the performance objective of  $7.2 \times 10^9$  storage capacity employing 1500 ft. of one inch wide tape with a packing density of 5,000 bits per inch per track on 80 tracks. Also, the machine showed excellent characteristics operating over a wide range of tape speeds. The basic design concept lends itself to growth and adaptation to a wide range of recorder requirements.

## TABLE OF CONTENTS

	<u>Page</u>
1. INTRODUCTION . . . . .	2-1
2. FIVE-YEAR HIGH RELIABILITY TAPE . . . . .	2-2
2.1 Configuration . . . . .	2-2
2.1.1 Reel Assembly . . . . .	2-5
2.1.2 Capstan Assembly . . . . .	2-5
2.1.3 Idler Assembly . . . . .	2-8
2.2 Control Systems . . . . .	2-10
2.2.1 Introduction . . . . .	2-10
2.2.2 General . . . . .	2-10
2.2.3 Speed Control System . . . . .	2-11
2.2.3.1 Speed-Capstan Drive Servo . . . . .	2-11
2.2.3.2 Tachometer Processing . . . . .	2-15
2.2.3.3 Speed-Command Generator . . . . .	2-16
2.2.4 Tension Control System . . . . .	2-16
2.2.4.1 Reel-Drive Servos . . . . .	2-16
2.2.4.2 Tension-Capstan Control . . . . .	2-21
2.2.4.3 Tension-Command Exciter . . . . .	2-21
2.2.4.4 Drag-Compensation Exciter . . . . .	2-21
2.2.4.5 Power-Off Dynamic Braking . . . . .	2-22
2.2.5 Mode-Control System . . . . .	2-22
2.2.6 Transport Circuitry . . . . .	2-25
2.2.7 Power System . . . . .	2-26
2.3 Design Parameters . . . . .	2-26
2.3.1 Life . . . . .	2-26
2.3.2 Guidance . . . . .	2-28
3. DESIGN ANALYSIS . . . . .	2-29
3.1 Tape Stresses . . . . .	2-29
3.1.1 Pack Stresses . . . . .	2-29
3.1.2 Tape Stresses Over Capstans . . . . .	2-32

TABLE OF CONTENTS (cont.)

	<u>Page</u>
3.1.3 Capstan Wrap Angle . . . . .	2-32
3.1.4 Tape Stresses Over Crowned Idlers . . . . .	2-32
3.1.5 Head Stresses and Pressure . . . . .	2-39
3.1.6 Free Length Tape Stresses . . . . .	2-42
3.1.7 Tape Stress Summary . . . . .	2-43
3.2 Guidance Analysis . . . . .	2-43
3.3 Natural and Induced Frequencies . . . . .	2-47
3.4 Kinetic Properties . . . . .	2-49
3.5 Bearings . . . . .	2-55
3.6 System Response . . . . .	2-59
4. TRANSPORT TESTS . . . . .	2-66
4.1 Tracking Accuracy . . . . .	2-66
4.2 Rotational Accuracies . . . . .	2-70
4.3 Flutter and Skew . . . . .	2-72
4.4 System Resonances . . . . .	2-79
4.5 Conclusions . . . . .	2-80



LIST OF TABLES

<u>Table</u>		<u>Page</u>
3.1	FEASIBILITY MODEL, FIVE YEAR RECORDER STRESSES OVER CYLINDRICAL CAPSTANS . . . . .	2-33
3.2	DOUBLE CONED IDLER STRESSES . . . . .	2-38
3.3	PARAMETER VALUES USED IN GUIDANCE ANALYSIS . . . . .	2-46
3.4	CALCULATED ATTENUATION VALUES FOR INDIVIDUAL IDLERS . . . . .	2-48
3.5	SYSTEM ATTENUATION VALUES . . . . .	2-48
3.6	BEARING SPECIFICATIONS . . . . .	2-56
3.7	BEARING LIFE DATA . . . . .	2-58
3.8	PHYSICAL PARAMETERS FOR TAPE RESPONSE COMPUTATION . . . . .	2-62
3.9	CALCULATED TAPE RESPONSE AT THE HEAD FOR FIVE- YEAR RECORDER . . . . .	2-62
3.10	COMPUTED VALUES OF JITTER . . . . .	2-65
4.1	SUMMARY OF TAPE TRACKING ACCURACY TESTS . . . . .	2-68
4.2	ROTATIONAL ACCURACY . . . . .	2-71
4.3	FLUTTER AND SKEW . . . . .	2-73-74
4.4	FLUTTER SPECTRUM . . . . .	2-77-78
4.5	TRANSPORT NATURAL RESONANCES . . . . .	2-81

## LIST OF FIGURES

<u>Figure</u>		<u>Page</u>
2.1	DECK LAYOUT . . . . .	2-3
2.2	ISOMETRIC OF TRANSPORT . . . . .	2-4
2.3	REEL ASSEMBLY . . . . .	2-6
2.4	DRIVE CAPSTAN . . . . .	2-7
2.5	ADJUSTABLE IDLER . . . . .	2-9
2.6	BLOCK DIAGRAM OF SPEED - CONTROL SERVO . . . . .	2-12
2.7	BASIC CIRCUIT OF TRANSCONDUCTANCE POWER- AMPLIFIER AND DC MOTOR . . . . .	2-14
2.8	BLOCK DIAGRAM OF EACH TENSION - CONTROL SERVO . . . . .	2-17
2.9	BLOCK DIAGRAM OF EACH REEL TORQUE - CONTROL SERVO . . . . .	2-19
3.1	TAPE PACK SIZE . . . . .	2-30
3.2	ACTUAL TAPE PACK STRESS DISTRIBUTION . . . . .	2-31
3.3	TENSION SLIP RATIO FOR CAPSTANS . . . . .	2-34
3.4	TAPE STRESS DISTRIBUTIONS OVER CROWNED ROLLERS . . . . .	2-35
3.5	EFFECTS OF ROUND-OFF . . . . .	2-37
3.6	HEAD PRESSURE STUDY . . . . .	2-40
3.7	HEAD STRESS STUDY . . . . .	2-41
3.8	TAPE STRESS PROFILE . . . . .	2-44
3.9	DOUBLE-CONED IDLER GUIDANCE MODEL . . . . .	2-45
3.10	SYSTEM NATURAL AND INDUCED FREQUENCIES ABOVE 10 HZ . . . . .	2-50
3.11	TAPE PACK RADIUS VERSUS LENGTH . . . . .	2-52

LIST OF FIGURES (cont.)

<u>Figure</u>		<u>Page</u>
3.12	TORQUE DEVELOPED BY TAPE TENSION . . . . .	2-52
3.13	REEL SPEED DURING RECORD MODE (3 ips) . . . . .	2-53
3.14	REEL SPEED DURING PLAY MODE (72 ips) . . . . .	2-53
3.15	TAPE PLUS REEL INERTIA . . . . .	2-54
3.16	TAPE PLUS REEL KINETIC ENERGY . . . . .	2-54
3.17	RELATIONSHIP BETWEEN ECCENTRICITY AND TORQUE EXECUTION MAGNITUDE . . . . .	2-60

FEASIBILITY MODEL OF A  
HIGH RELIABILITY FIVE-YEAR TAPE TRANSPORT

1. INTRODUCTION

The scope of Volume II includes discussions relating to the details of the design, the application of the analytical models, the reliability assessment, and details of the tests performed on the transport. In an effort to make this presentation as clear as possible, a number of elements which are peripheral to the main objective are presented in separate appendices in Volume III.

## 2. FIVE-YEAR HIGH RELIABILITY TAPE TRANSPORT

### 2.1 Configuration

The Five-Year High Reliability Transport is a reel-to-reel coplanar configuration with independently motor driven reels and capstans. This coplanar configuration was selected after evaluating other types of tape handling systems (see Phase I Final Report).<sup>1</sup> Evaluation factors included consideration of:

- Long life
- Reliability
- Simplicity
- Package size and weight
- Modularization
- Tape guidance
- Assembly and test procedures
- Flight requirements

The deck layout of the IITRI configuration is shown in Figure 2.1. An isometric of the transport is shown in Figure 2.1A. The reel spacing allows for up to 1600 feet of 1 mil thick tape. The capstan and idler locations were selected to give reasonably large lead-in tape lengths to each of the crowned idlers. Large lead-in lengths were found beneficial to tape guidance. The layout also provides large wrap angles ( $165^\circ$  and  $180^\circ$ ) around the two capstans and clearance space for the record head. A straight length of tape for mounting the erase head and noncontacting end-of-tape sensor is also provided. Furthermore, the oxide tape surface does not contact either crowned idler. This minimizes debris and wear problems.

The deck occupies an area of approximately 169 inches<sup>2</sup> and the entire transport can easily be packaged in a 13 x 13 x 15 inch volume.

---

1. "Design Study for a High Reliability Five-Year Spacecraft Tape Transport," G. S. L. Benn and Dr. R. L. Eshelman, for NASA/Goddard Space Flight Center, Greenbelt, Md., Contract No. NA55-21556, Nov. 1971.

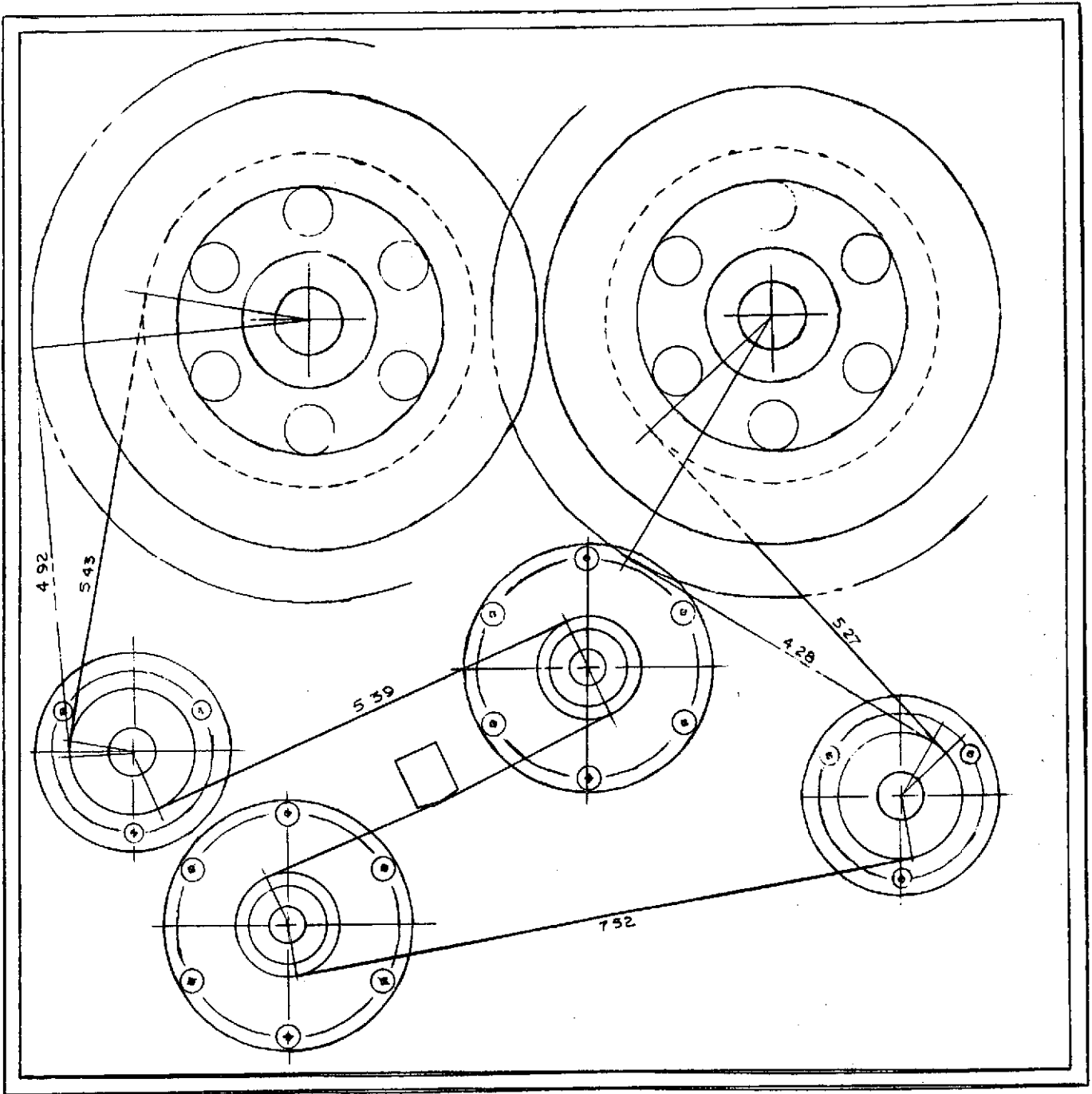


Figure 2.1 DECK LAYOUT

1

2

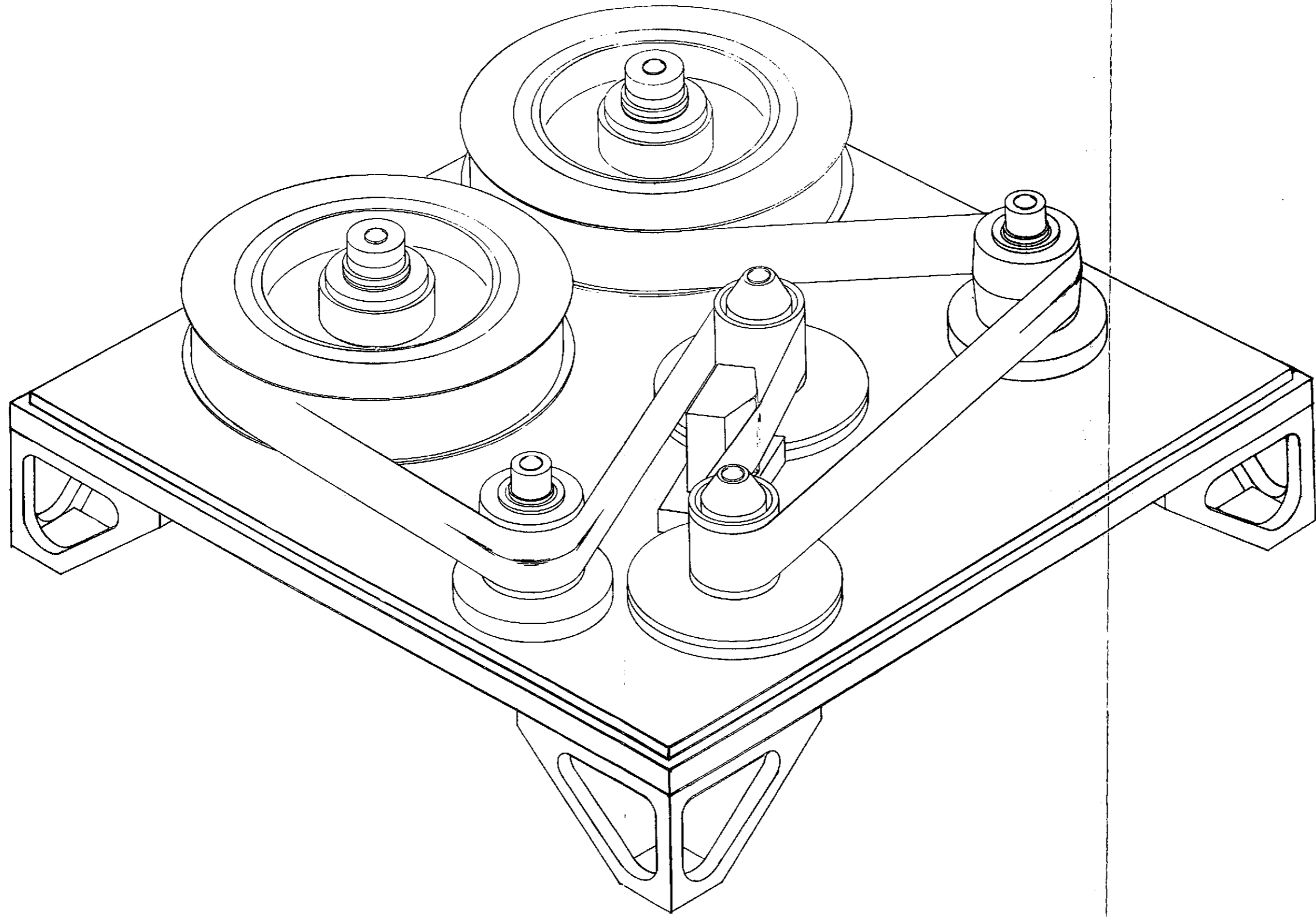


Figure 2.2 ISOMETRIC OF TRANSPORT

An aluminum mounting deck is used in the construction of the feasibility model. This deck has a thickness of 0.625 inches and is accurately machined to accept the modules.

#### 2.1.1 Reel Assembly

Storage of the magnetic tape is provided by the reel assembly shown in Figure 2.3. The reel assembly is an independent module that includes the reel, a reel support structure and bearings, dust seals, and a DC\* drive motor. This compact configuration is obtained by directly attaching the DC motor armature to the reel. The DC motor field housing is an integral part of the module's support housing. Substantial bearings of the Precision Class are preloaded to a 24 ounce level by using a calibrated preload spring technique. Preloadings are employed to assure effective bearing performance, as well as to minimize the run-out effects resulting from internal bearing clearances. Reel shaft run-out errors are directly translated into gross tape tracking errors. To minimize these reel generated tracking errors, preloading and precision mechanical assembly procedures are employed to control reel hub run-out to less than  $\pm 0.0005$  inches.

The bearing preload is applied by a wave washer. The load deflection curve of the washer is first measured to determine the required compressed height. During assembly, the distance from the bearing cap to the top of the reel shaft is accurately measured. The shim height can then be lapped to the required thickness and an accurate preload is assured.

#### 2.1.2 Capstan Assembly

The capstan assemblies as shown in Figure 2.4 provide for low and high speed tape metering. Both assemblies utilize direct drive DC motors to control the tape in the vicinity of the head and

---

\* DC-brush/commutated motors were employed because of developmental cost constraints. Advanced models may be fitted with DC-brushless motors.



E6725-C-0150

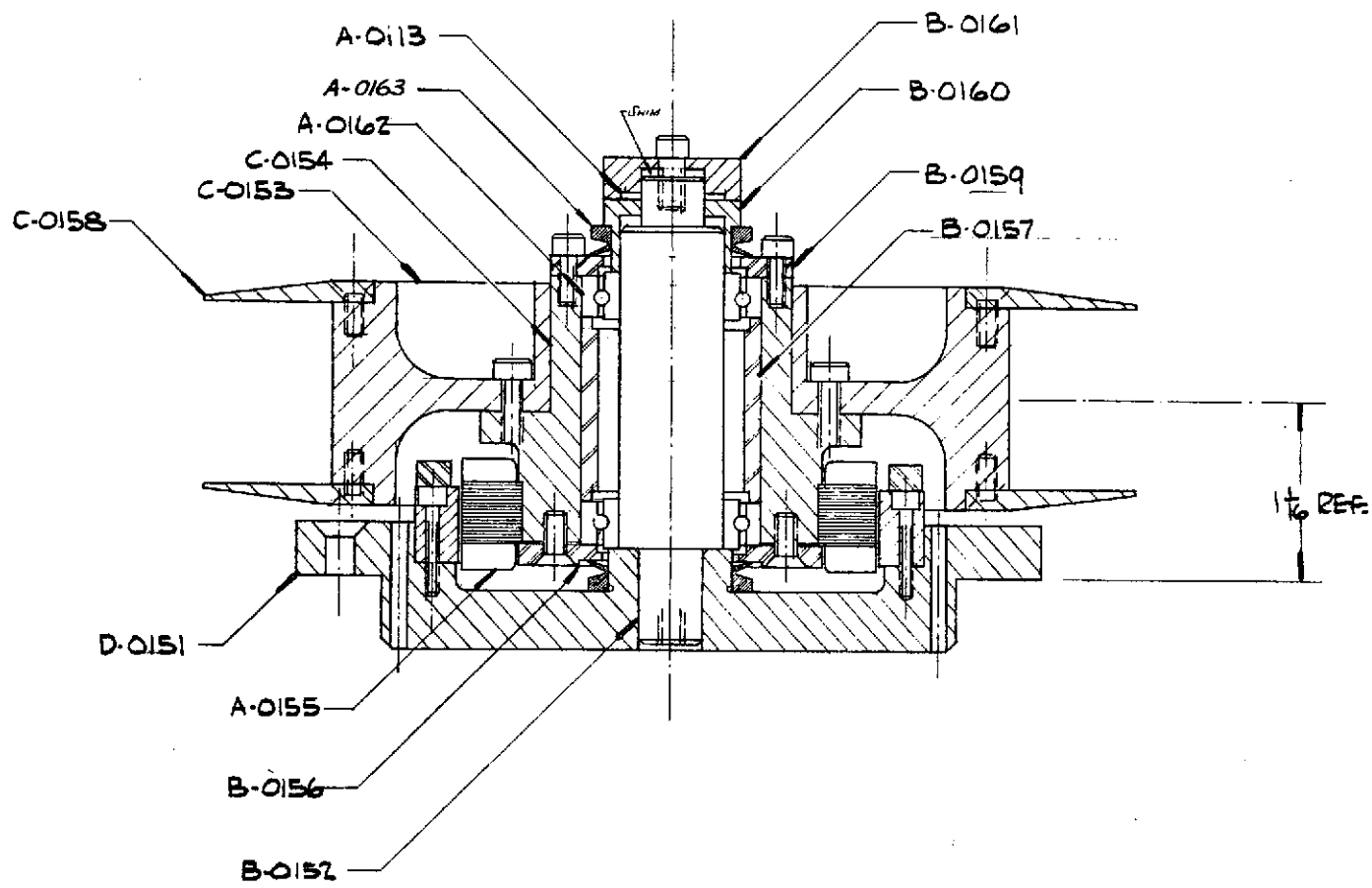


Figure 2.3 REEL ASSEMBLY

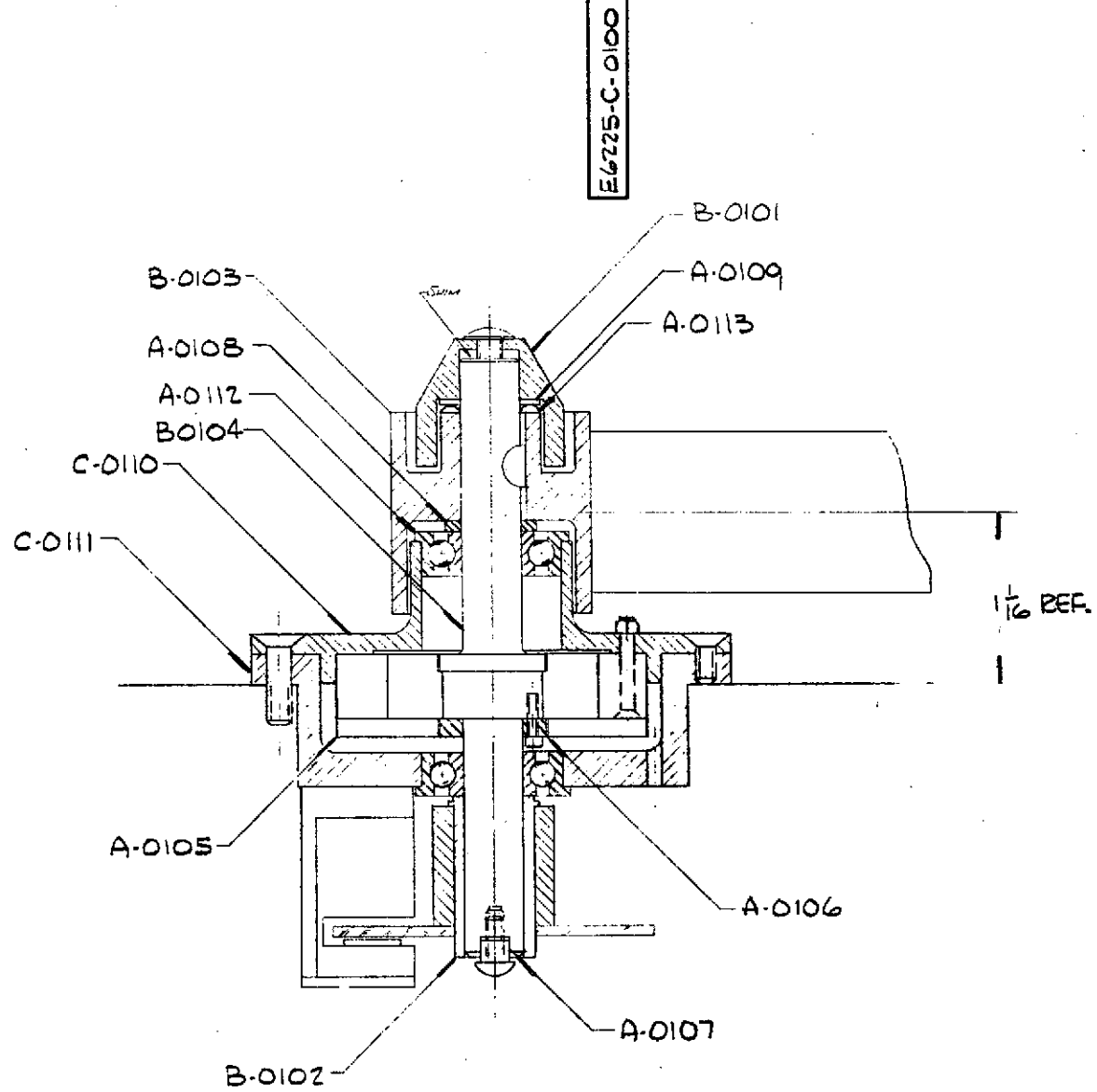


Figure 2.4 DRIVE CAPSTAN

to mechanically filter tape propagated disturbances. The DC motors induce damping from the electrical field and help to control tensions through drive or drag (back emf).

The capstans are driven directly by DC motors with the motor armatures mounted directly on the capstan shafts. The driven shafts are mounted to a structure that attaches to the tape deck through ball bearings.

The bearing preload, which is set at 16 ounces, is achieved by shimming. The technique is similar to that described in preloading the reel bearings.

The capstan surfaces were case with a Conthane elastomer and machined to a fine tolerance. This material gives an extremely high friction coefficient and exhibits excellent wear properties. The thickness of this bonded elastomer is approximately 0.032 inches.

### 2.1.3 Idler Assembly

Tape guidance is performed by two of the double coned idler assemblies as shown in Figure 2.5. The idler collars are 1.5 inches in diameter and have a 2 degree cone angle. The apex of the roller is rounded with a 3 inch radius. This radius reduces the stress level at the tape centerline but allows the roller to guide as a double cone.

The double coned roller rotates around a support post through two precision bearings. Bearing preload (16 ounces) is obtained with a wave washer and established by shimming. The support post is integrally mounted to the idler housing. Perpendicularity is achieved by maintaining a close control between the housing and the deck plate surface.

E6275-C-0175

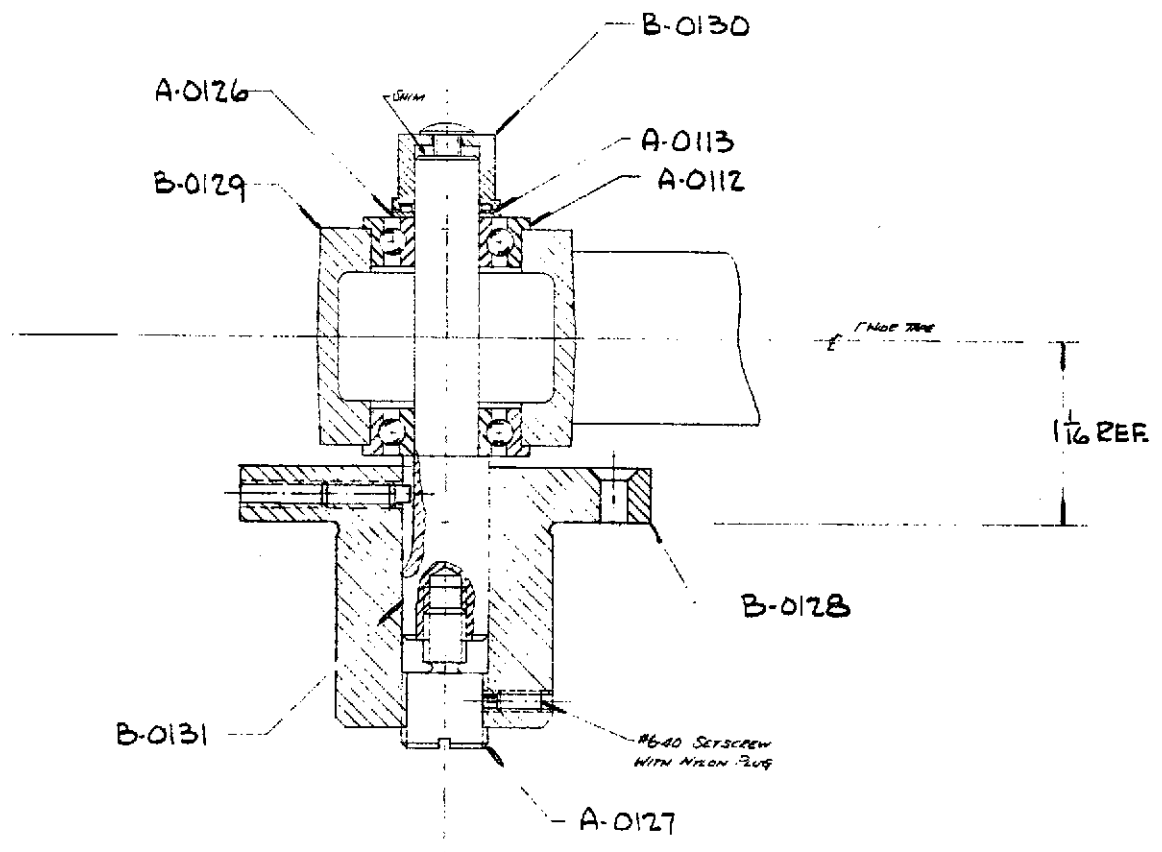


Figure 2.5 ADJUSTABLE IDLER

A differential screw mounted to the bottom of the support post allows accurate vertical adjustment of the idler. A set-screw is provided to retain the fine adjustment. This fine adjustment allows control of the dynamic equilibrium position of the tape.

## 2.2 Control Systems

### 2.2.1 Introduction

The major emphasis or goal of the design study\* on which the design of the Five-Year Transport is based was that of achieving long mechanical life with minimum consideration of size, weight, power consumption, and the required associated control systems. Thus, the transport is intended to serve primarily as a "test bed" for both proving the long-life design concepts and guidelines established in the design study, and evaluating various configuration options, rather than either being a prototype or representing the ultimate in overall performance. In view of this, the control systems incorporated into the transport were designed for versatility and gentle tape handling along with the best performance that could be readily achieved using simple control loops, with essentially no consideration of size or power consumption.

### 2.2.2 General

The basic control functions required for the transport are tape speed control, tape tension control and mode control. Independent control of both average speed and tension could be effected with just two motors, one driving each reel; but to

---

\* IIT Research Institute, "Design Study for a High Reliability Five-Year Spacecraft Tape Transport," Final Report, November 1971, Project No. E6179, for Goddard Space Flight Center, Contract No. NAS5-21556.

provide better control of instantaneous tape speed at the head, a third motor driving a capstan (henceforth called the speed capstan) near the head is used for speed control. Finally, a fourth motor driving a second capstan (henceforth called the tension capstan), on the other side of the head, is used for versatility to permit the tape tensions at the two reels and the head to all be independently controlled.

To provide mechanical simplicity and compactness, "pancake" style motors are used with their armatures directly mounted on the elements they drive. The motors are DC brush type with permanent-magnet fields. This choice was dictated by funding limitations and on the basis of good efficiency and expedience, such as ease of driving. Finally, to further reduce temperature rise and provide more power-off dynamic-bracking torque (see section 2.2.4.5), oversized motors are used. Detailed control system operation is given in Appendix F of Volume III.

### 2.2.3 Speed Control System

#### 2.2.3.1 Speed-Capstan Drive Servo

Tape speed is maintained at a commanded value, independent of friction and tape tension, by a closed-loop control system which continuously adjusts the drive to the speed-capstan motor to maintain the proper capstan rotation rate. This closed-loop control system constitutes a type-II\* velocity servo and is shown in block-diagram form in Figure 2.6.

Capstan rotation rate is measured with an optical pulse-rate tachometer (also variously called: digital tachometer, incremental encoder, or quantizer) which consists of a 2500-line

---

\*Denotes that the net number of integrations around the loop is two.

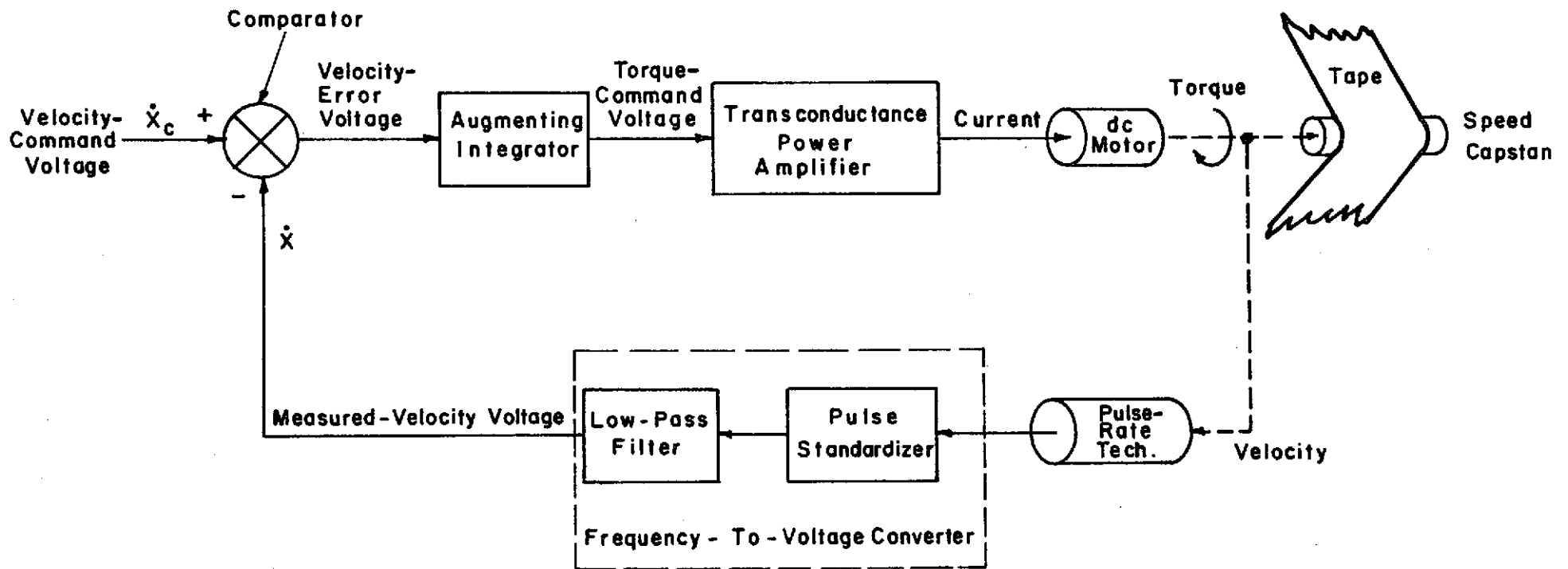
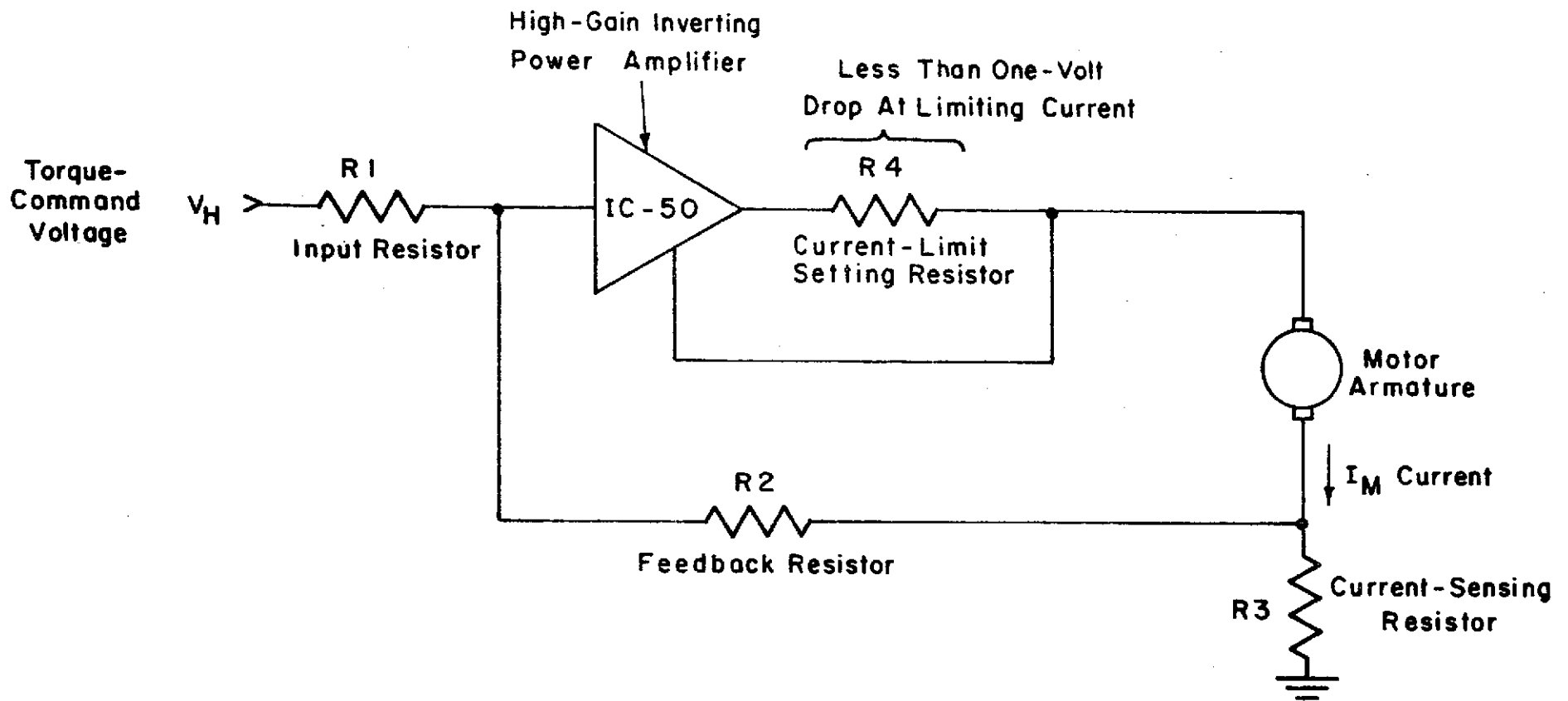


Fig. 2.6 BLOCK DIAGRAM OF SPEED - CONTROL SERVO

radially-ruled glass disk, mounted on the lower end of the speed-capstan shaft, and an adjacent stationary photoelectric sensing head. The pulse rate from the tachometer, which is proportional to capstan and tape speeds, is converted to a proportional voltage in a frequency-to-voltage converter. This latter voltage is then compared to the input velocity-command voltage to produce a velocity-error voltage. This velocity-error voltage is then integrated (at frequencies below 70 Hz) or amplified (at frequencies above 70 Hz) to form the torque-command voltage. Finally, the transconductance power amplifier drives a current through the motor that is proportional to the torque-command voltage, and the motor develops a torque proportional to its current. The power amplifier is forced, using the basic circuit shown in Figure 2.7, to deliver an output current, rather than voltage, proportional to its input voltage to make motor torque independent of motor speed and armature-winding resistance.

When the servo is unloaded (i.e., speed-capstan not in contact with tape), there is an inherent  $90^\circ$  phase lag between changes in motor current or torque and the resulting changes in capstan velocity. Since the only other source of significant phase shift around the loop at moderate frequencies is the low-pass filter in the frequency-to-voltage converter, it follows that the maximum bandwidth that can be achieved by the servo, with reasonable stability margins, is limited to some fraction of the frequency at which the filter exhibits a  $90^\circ$  phase lag. For a given filter type, this  $90^\circ$  lag frequency is directly related to the filter cut-off frequency and this, in turn, is determined by the maximum permissible filter output ripple at the lowest operating pulse rate from the tachometer. The tachometer circuitry produces 5000 pulses per revolution and the capstan has a diameter of 1.25 inches, so  $5000/(1.2511)\pi$  or 1272.12 pulses are produced per longitudinal inch of 0.0011-inch thick tape. Thus at the lowest operating tape speed of three inches per second, the rate is (3) (1277.12) or about





For  $R2 \gg R3$  :  $I_M = V_H \frac{-R2}{R1 R3}$

Fig. 2.7 BASIC CIRCUIT OF TRANSCONDUCTANCE POWER AMPLIFIER AND DC MOTOR

3816 per second. Acceptable attenuation (about 46 dB) of this lowest ripple frequency is provided by use of a four-pole low-pass Butterworth-type active filter having a cut-off frequency of 1000 Hz. Such a filter exhibits a phase lag of  $180^\circ$  at 1000 Hz, and  $90^\circ$  at about 570 Hz. Consequently, the servo provides an unloaded bandwidth of about 350 Hz with reasonable stability margins.

The integrator was incorporated into the loop to provide essentially perfect steady-state speed regulation with regard to load torque or tape tension. Consequently, the steady-state or average speed of the capstan and tape is independent of tape tension up to the torque limit of the motor. However, the  $90^\circ$  phase lag of a simple integrator would make the loop unstable, so the integrator is augmented with a lead corner at 70 Hz to nullify the integration and its phase lag at frequencies above 70 Hz. A complete schematic circuit diagram of the speed-control circuit which includes the augmenting integrator and transconductance power amplifier, is shown in Figure F-1 of Volume III.

#### 2.2.3.2 Tachometer Processing

The principal functions of the tachometer processing circuitry are those of producing an analog voltage accurately proportional to the pulse rate from the tachometer, and a binary switching signal defining the direction of capstan rotation (and, thus, direction of tape travel). The optical tachometer (Litton Model MBI500-2500G3) produces two output square-wave signals, A and B, each having 2500 cycles per revolution, but differing in phase by about  $90^\circ$  to provide direction information. In the forward (record) direction, A leads B by  $90^\circ$ , while in the reverse (play) direction, A lags B by  $90^\circ$ . The processing circuitry thus contains a frequency-to-voltage converter and a digital phase-polarity detector. A complete schematic circuit diagram of the tachometer processing circuitry is presented in Figure F-2, Volume III.

### 2.2.3.3 Speed-Command Generator

The basic purpose of the speed-command generator is simply that of providing convenient means for manually adjusting the command-input voltage ( $-\dot{X}_c$ ) to the speed-control servo over ranges corresponding to about 2 to 10 inches per second, and about 20 to 80 inches per second. Both ranges are provided in the forward (record) direction, while only the fast range is provided in the reverse (play) direction. The maximum rate at which  $-\dot{X}_c$  may change is precisely limited to provide smooth and gentle tape handling. This rate limiting of the speed command is normally set to yield a maximum tape acceleration of  $\pm 14.4$  inches/sec<sup>2</sup> so that a speed change from zero to 72 inches/sec (or 72 inches/sec to zero) requires five seconds. A complete schematic circuit diagram of the speed-command generator is presented in Figure F-3. Volume III.

### 2.2.4 Tension Control System

Tape tension at each of the two reels is independently established by its own control system; while tape tension at the head simply equals (neglecting friction) the tension at the left reel, plus or minus an adjustable tension increment introduced by the tension capstan.

#### 2.2.4.1 Reel-Drive Servos

Tape tension at each reel is maintained at a commanded value in the range of 4 to 13 ounces, independent of friction, reel-rotation rate, tape-pack radius, and tape speed (except when variation with tape speed is desired), by a closed-loop control system which continuously adjusts the drive to its reel motor to develop the proper torque. This closed-loop control system constitutes a type-I\* tension servo and is shown in block-diagram form in Figure 2.8. To offer testing versatility, a switch is provided which permits transforming

---

\*Denotes that the net number of integrations around the loop is one.

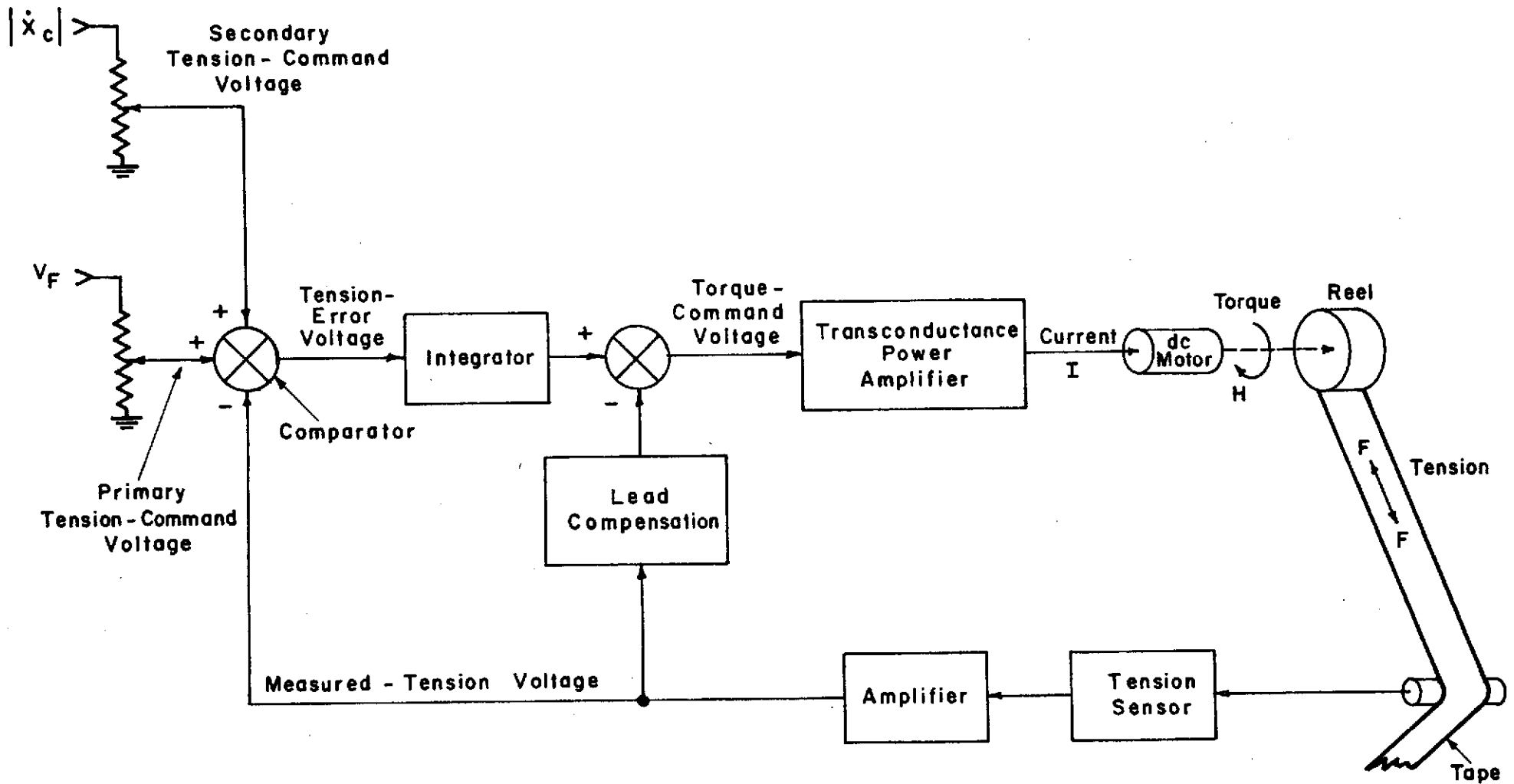


Fig. 2.8 BLOCK DIAGRAM OF EACH TENSION - CONTROL SERVO

each servo to a simple open-loop torque control system, providing a range of about 12 to 40 ounce-inches, whose block diagram is shown in Figure 2.9.

Tape tension for each reel-drive servo is measured with a separate instrument (Minnetech Model MTM106) which determines tape tension by sensing the bearing-reaction force on a freely-rotating idler that deflects the tape path. The tension-sensing idler (and its force transducer) for the left reel-drive servo is located between the left crowned roller and the tension capstan, while the tension-sensing idler (and its force transducer) for the right reel-drive servo is located between the right crowned roller and the speed capstan. The output of each tension sensor is amplified and compared to the input tension-command voltage (which has two components) to produce a tension-error voltage which then is integrated to form the major portion of each servo's torque-command voltage. Finally, each transconductance power amplifier drives a current through its motor that is proportional to its torque-command voltage, and the motor develops a torque proportional to its current. Each power amplifier is forced, using the basic circuit shown in Figure 2.7, to deliver an output current, rather than voltage, proportional to its input voltage to make motor torque independent of motor speed and armature-winding resistance.

Due to the moment of inertia of each reel with its motor and stored tape, and the compliance of the tape between each reel and the speed capstan (which can be considered rigid for a first approximation), the open-loop transfer function between the torque or current of each motor and the output of its associated tension sensor exhibits a lightly-damped resonance in the neighborhood of 14 to 25 Hz, depending on tape-path length and amount of tape stored on each reel. To provide stable operation of the reel-drive servos with such resonances within their closed loops, a portion of each measured-tension voltage is also fed back to its transconductance power amplifier through

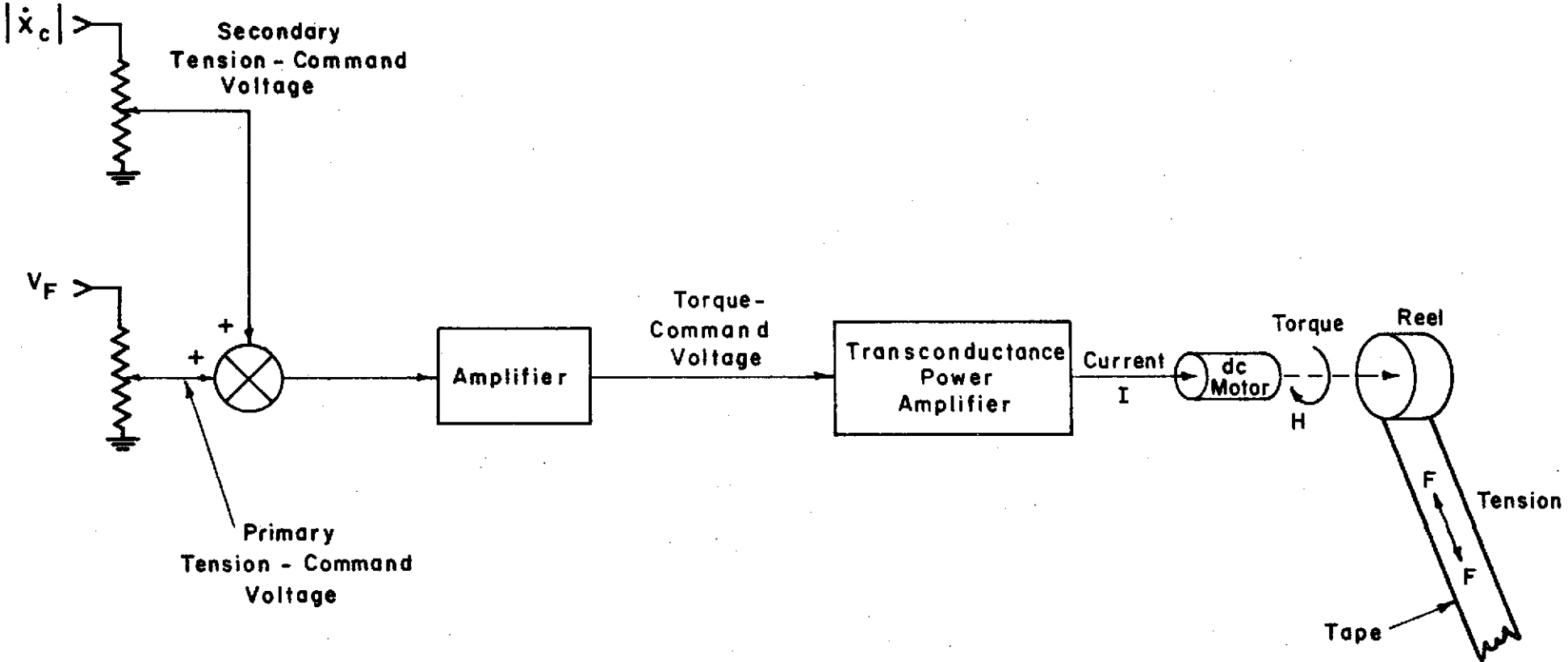


Fig. 2.9 BLOCK DIAGRAM OF EACH REEL TORQUE - CONTROL SYSTEM

a phase-lead compensation network (high-frequency-limited differentiator) to produce electrical damping of the mechanical resonances. However, the addition of this damping does not alter the  $90^\circ$  phase lag that occurs at the natural frequency of each resonance, so in view of the  $90^\circ$  phase lag of the integrator, the closed-loop bandwidth of the reel-drive servos is, for stability, restricted to something less than these mechanical natural frequencies.

The integrator was incorporated into the loop to provide essentially perfect steady-state tension regulation with regard to tape-pack radius friction and other disturbance variables.

The primary tension-command voltage is a manually-selected portion of a voltage,  $V_F$  which is +10 volts when the tape is moving and zero when the tape is stationary (standby mode) To provide gentle tape handling,  $V_F$  is not simply switched between zero and +10 volts but, rather, is produced by a tension Command Exciter which causes  $V_F$  to change slowly from 0 to +10 (at turn on) and -10 to zero (at turn off) at controlled rates. The secondary tension-command voltage is a manually-selected portion of a voltage,  $\left| \dot{X}_C \right|$ , which is approximately proportional to the magnitude of the commanded tape speed. This secondary tension command is provided to permit having tape tension increase as a linear function of tape speed (magnitude).

A complete schematic circuit diagram of the left-reel control which includes all components of the left-reel-drive servo except for the motor and tension sensor. is shown in Figure F-4, Vol. III. The right-reel control is identical except  $V_D$  is replaced by  $-V_D$  and all part numbers are increased by 300 (i.e., numbers in the 500's), so it will not be discussed further.

#### 2.2.4.2 Tension-Capstan Control

The tension capstan introduces a fixed tension increment that is adjustable over a range from -8 to +8 ounces and is independent of tape speed. Since the capstan has a diameter of 1.25 inches, this tension-increment range is provided by developing a constant torque adjustable from -5 to +5 ounce inches. This is achieved with a simple open-loop control arrangement in which the capstan motor is driven by the current from a transconductance power amplifier whose input (torque-command voltage) is a manually-selected fraction of the  $V_F$  voltage. A complete schematic circuit diagram of the tension-capstan control is shown in Figure F-6, Vol. III.

#### 2.2.4.3 Tension-Command Exciter

The purpose of the tension-command exciter is that of providing gentle tape handling by causing tape tension to smoothly vary at a controlled rate during mode transitions, from near zero when the tape is stationary to the full commanded values when the tape is moving. This is accomplished by producing a voltage,  $V_F$ , which slowly changes in from 0.5 to 2 seconds (adjustable) from zero to +10 volts when the tape starts moving, and from +10 volts to zero when the tape stops moving, and using this voltage to excite the three manually-set tension-command potentiometers (on left and right reel-control panels, and tension-capstan control panel). A complete schematic circuit diagram of the tension-command exciter is shown in the upper portion of Figure F-7, Vol. III.

#### 2.2.4.4 Drag-Compensation Exciter

The purpose of the drag-compensation exciter is to produce a voltage,  $V_D$ , from which the four motor drives can derive offsets to compensate for their friction drags so that their torque-command inputs will be accurately proportional to their



respective net useful output torques. Since most of the drag at each motor appears to be brush/commutator coulomb friction,  $V_D$  is simply made +10 volts when the tape is moving forward (record), -10 volts when the tape is moving backward (play), and zero in the standby mode. This is accomplished by the circuitry depicted schematically in the lower portion of Figure F-7, Vol. III.

#### 2.2.4.5 Power-Off Dynamic Braking

To eliminate or minimize the possibility of "throwing a loop" or otherwise snarling the tape when power is lost while the tape is moving at high speed, a drag torque (opposing tape motion) proportional to reel-rotation rate is produced by only the supply reel (the one from which tape is being unwound) immediately after power is lost and continues until the tape stops. This action is achieved by the simple expedient of shorting the armature of the supply-reel motor when power is lost to develop dynamic braking. A schematic of how this is accomplished is shown in Figure F-10, Vol. III.

#### 2.2.5 Mode-Control System

The mode-control system consists of most of the logic and switching operations necessary for executing orderly transitions between the record, play, and standby modes selected in any sequence. Some of the principal features of this system are:

1. Mode-selection push-buttons and relays are electrically interlocked to prevent inadmissible or contradictory states if two or more buttons are pressed at the same time or if a relay releases slowly.
2. When switching from either record or play to standby, the primary component of tape tension (see section 2.2.4.1) is maintained and the speed-capstan drive servo (see section 2.2.3.1) is kept operating until tape speed drops below

about 1.6 inches/second.

3. End of tape is sensed electro-optically with detectors viewing infrared light sources through "windows" in the tape near each end.
4. Electronic latching of the outputs of the end-of-tape sensors is employed to permit use of very narrow "windows" (as opposed to the very long windows that would be required by the high tape speed and relatively long relay action time if the sensors were to control relays directly).
5. Switch selection of having the tape either stop or reverse direction (recycle) when either end of tape is reached.
6. If both end-of-tape sensors are operated at the same time (as when tape breaks, completely unwinds from either reel, or leaves its normal path), all power is shut off.

Delineation of the logic employed to achieve the above performance is most conveniently expressed in Boolean form. For this purpose, the following input variables are first defined:

<u>INPUT VARIABLE OR CONDITION</u>	<u>SYMBOL</u>
Record push button (S1) pressed	$R_b$
Play push button (S2) pressed	$P_b$
Standby push button (S3) pressed	$S_b$
Record-mode relay (K1) operated (normally-open contacts closed)	$R_r$
Record-mode relay (K1) operated (normally-closed contacts closed)	$\overline{P_r^*}$
Play-mode relay (K2) operated (normally-open contacts closed)	$P_r$
Play-mode relay (K2) not operated (normally-closed contacts closed)	$\overline{P_r^*}$

INPUT VARIABLE OR CONDITION	SYMBOL
Left end-of-tape sensor not blocked by tape	$T_L$
Right end-of-tape sensor not blocked by tape	$T_R$
Left end-of-tape memory (latch) set	$M_L$
Right end-of-tape memory (latch) set	$M_R$
Operate memory (latch) set	$M_O$
End-of-tape action switch (S5) in "recycle" position	C
End-of-tape action switch (S5) is "stop" position	$\bar{C}$
Tape speed magnitude greater than 1.6 inches/sec	$V_1$

The output variables and the Boolean expressions defining the conditions under which these output actions occur (listed action occurs when Boolean expression is "true" or = 1) are:

OUTPUT VARIABLE OR ACTION	REQUIRED CONDITION
Energize record-mode (K1) relay	$\bar{S}_b \left[ \bar{P}_b (\bar{P}_r R_b + R_r \bar{M}_L) + C M_R \bar{P}_r \right]$
Energize play-mode (K2) relay	$\bar{S}_b \left[ \bar{R}_b (\bar{R}_r P_b + P_r \bar{M}_R) + C M_L \bar{R}_r \right]$
Set left end-of-tape memory	$R_r T_L$
Reset left end-of-tape memory	$R_b + \bar{R}_r \bar{C} + P_r C + P_r T_R$
Set right end-of-tape memory	$P_r T_R$
Reset right end-of-tape memory	$P_b + \bar{P}_r \bar{C} + R_r C + R_r T_L$
Set operate memory	$(R_r + P_r) V_1$
Reset operate memory	$\bar{V}_1$
Energize K401 (i.e., operate speed-capstan motor) and Tension-Command Exciter	$R_r + P_r + M_O$

A complete schematic circuit diagram of the mode-control system is shown in Figure F-8, Vol. III.

### 2.2.6 Transport Circuitry

All of the electromechanical components of the control systems are mounted on, or immediately adjacent to, the deck plate that forms the transport structure. These components consist of the two reel-drive motors: (each Magnetic Technology type 1937-050-115), the pulse-rate tachometer (Litton Model MBI 500-2500G3) mounted on the lower end of the speed capstan, the force transducers of the tension-sensing instruments (each Minnetech Model MTM 106), and the end-of-tape sensors (each General Electric Type H13B1).

The tension-sensors' force transducers are mounted on a removable acrylic plate spaced about two inches above the deck, with the left one located between the left crowned roller and the tension capstan, and the right one located between the right crowned roller and the speed capstan. The position of each transducer is such that its idler deflects the tape path  $9^\circ$  ( $18^\circ$  wrap angle), so that a tension of 15 ounces will produce a full-scale indication (0.6 volts output) on the associated tension-sensing instrument when the latter is set to its 10-ounce range (calibrated for  $15^\circ$  tape deflection, or  $30^\circ$  wrap angle, at zero tension).

Each of the end-of-tape sensors consists of an infrared light-emitting diode facing a photo-darlington transistor across a gap of about 1/8 inch. Both sensors are located between the head and the speed capstan, with the left sensor straddling the upper (away from deck) edge of the tape and the right sensor straddling the lower (toward deck) edge of the tape. The "windows" in the tape that are detected by these sensors are about 0.4-inch long and extend less than a third of the way across the tape (from top edge near left end, and from lower edge near right end of tape). These "windows" were made by dissolving the backing and oxide binder with methyl ethyl ketone,

and were placed about 25 feet from each end of the tape to allow a five-second deceleration from 72 inches/second with some margin to avoid running the tape off either reel. A complete schematic diagram is shown in Figure F-9, Vol. III.

### 2.2.7 Power System

The complete control system is powered by external power supplies providing +24 volts and -20 volts. These voltages are used directly for the power amplifiers and the +24 is also used directly for relays and lamps. All digital logic operates from +5 volts which is derived from the +24 volts by a three-terminal integrated-circuit voltage regulator (Fairchild Type UGH7805343) while all operational amplifiers and other analog-processing circuitry operates from +15 volts and -15 volts which are derived from the +24 volts and -20 volts respectively with integrated-circuit voltage regulators (Motorola Type MC1469R and MC1463R, respectively). A power relay and appropriate logic are employed which prevents voltage from being applied to any other circuitry unless both input voltages are present and have the proper polarities. The circuitry also prevents turning off the power (via the "off" push button) unless the equipment is in the standby mode, but provides (in conjunction with circuitry depicted in Figure F-8, Vol. III) immediate turn-off of all power if the tape breaks or comes off of either reel. A complete schematic circuit diagram of the power switching, regulators, and distribution is shown in Figure F-8, Vol. III.

## 2.3 Design Parameters

### 2.3.1 Life

The principal goal in the design of the IITRI transport has been the achievement of the "five-year life" requirement. The term "five-year life" used throughout this report is meant to represent continuous operation at 100 percent duty cycle over

a five-year period. A value of 10,000 tape passes per year has been assigned which is typical of earth orbital satellite requirements. Therefore the long life requirement of the tape transport may be defined as the ability to record and reproduce data successfully for 50,000 full tape passes. Since 1500 feet of record tape is used, 75 million feet of tape must pass over the record head. The total number of revolutions as seen by the capstans, idlers and reels are:

Capstans	=	2290 million revs
Idlers	=	1910 million revs
Reels	=	550 million revs

To meet these severe requirements, large bore precision ball bearings are used. In addition, a bearing preload scheme is used that insures and maintains an accurate preload throughout the useful life of the transport.

The long life requirement has dictated and influenced many of the transport design decisions. Modularization and simplicity of components is perhaps the most obvious. In fact, only three different pairs of elements, namely reels, capstans and idlers, comprise the entire tape handling system.

Equally important to the achievement of long life has been the elimination of historically unreliable mechanical elements. In particular, the IITRI transport utilizes no belts, negator springs, differentials or gears. In fact, the only life-limiting mechanical elements utilized are bearings and motors.

### 2.3.2 Guidance

The tape handling elements of the transport have the obvious but important function of moving the tape across the head at a controlled velocity and along a fixed path. The ability of the transport to prevent lateral excursion of the tape from the mean path is generally referred to as guidance. Furthermore, the record capability of a machine is directly related to the number

of tracks across the tape. Increasing the number of tracks, however, demands a decrease in the track width. Narrow track widths, in turn, require extremely accurate tape guidance to prevent signal loss during play.

Three types of guidance elements were initially considered for the "five-year" transport. The first of these types involved flanged rollers. This type, however, was eliminated from further consideration on the basis that adequate tape tracking could not be obtained with a wide (1 inch) tape. Secondly, laboratory measurements showed that tape edges are extremely jagged, as a result of slitting, and unsuitable for accurate tracking. Furthermore, edge guiding results in excessive debris formation and can lead to early tape failure.

The remaining two types of guidance elements considered were a double coned idler and a spherically crowned idler. Extensive parameter variation studies using the IITRI stress and guidance programs resulted in the selection of two double-coned idlers modified with a spherical round-off. This hybrid roller exhibits the excellent tracking ability of a double-coned roller without inducing high tape stress at the centerline.

### 3. DESIGN ANALYSIS

#### 3.1 Tape Stresses

A major requirement for the successful operation of a long life satellite recorder is the ability of the tape to withstand the mechanical stresses imposed. Consequently IITRI has spent considerable effort in developing a highly sophisticated computer program capable of calculating various roller induced stress values within the tape. A discussion of this program is given in Appendix C, Volume III.

There are two principal areas in which mechanical stresses are induced in the magnetic tape; namely, those stresses generated within the tape pack and secondly those stresses resulting from bending around capstans, idlers and heads. In order to establish and verify the IITRI transport tape handling design, a complete stress analysis of the tape has been conducted. A discussion of these analyses and the resulting stress profile, as seen by the tape, is herein presented.

##### 3.1.1 Pack Stresses

Evaluating the pack radius for various hub diameters and tape lengths yields the curves shown in Figure 3.1. Fifteen hundred feet of tape wrapped on a four inch diameter hub have been selected for the feasibility model. The number of wraps for 1500 ft. of tape will be of the order of 1100 wraps. Additional tape (50 to 100 ft.) is provided for lead-in and end of tape sensing.

The 4 in. reel hub diameter and hub stiffness was arrived at by conducting a trade-off study which showed that a stable tape pack will result for 8 to 12 oz. of tape tension. Furthermore, a radial hub thickness of 0.75 inches is adequate to provide the necessary stiffness beneath the tape pack. A 4 inch diameter aluminum hub was selected for the feasibility model.

The calculated tape pack stresses for a winding tape tension of 10 oz. are shown in Figure 3.2. All of the stresses are tensile.



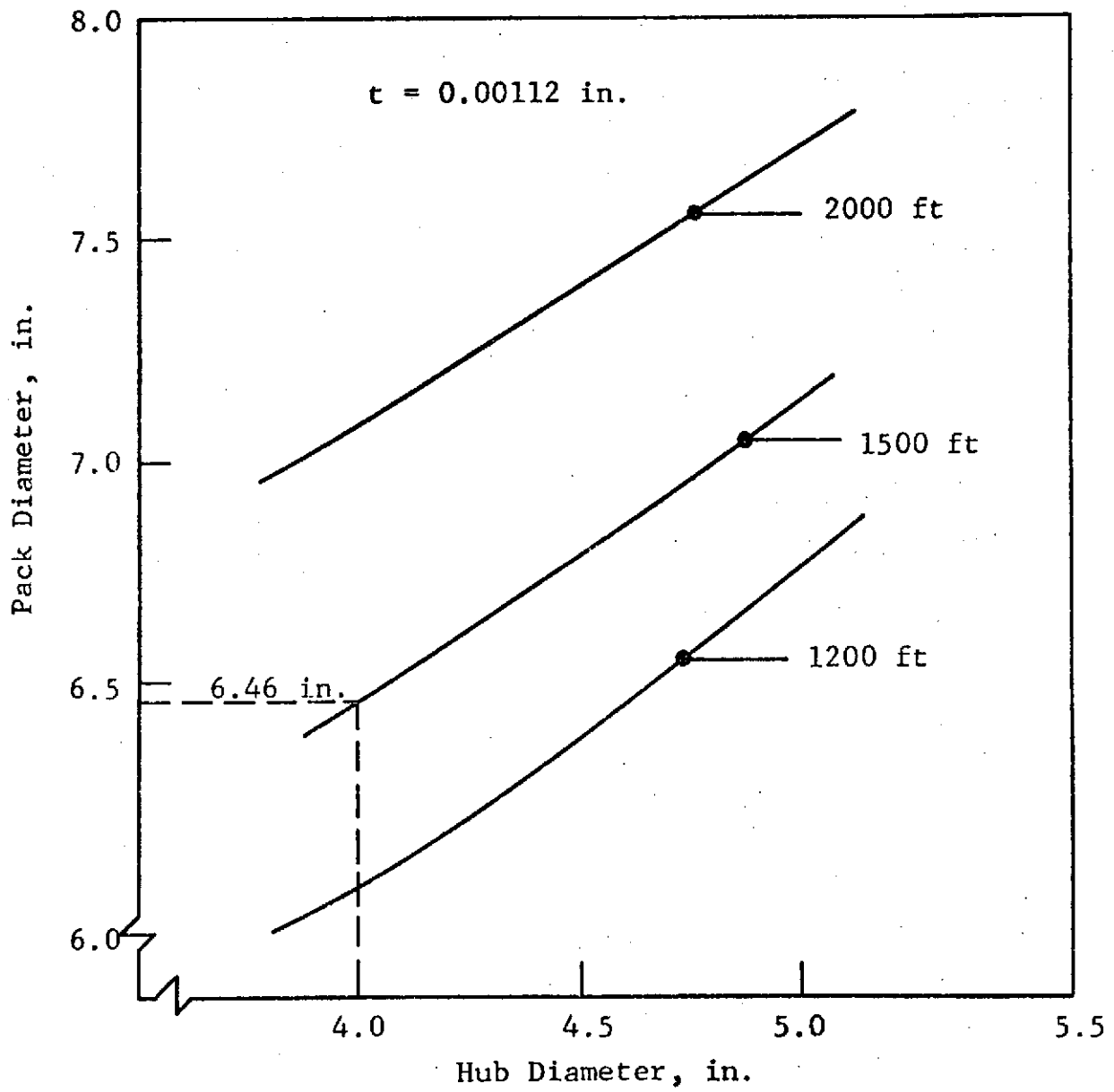


Figure 3.1 TAPE PACK SIZE

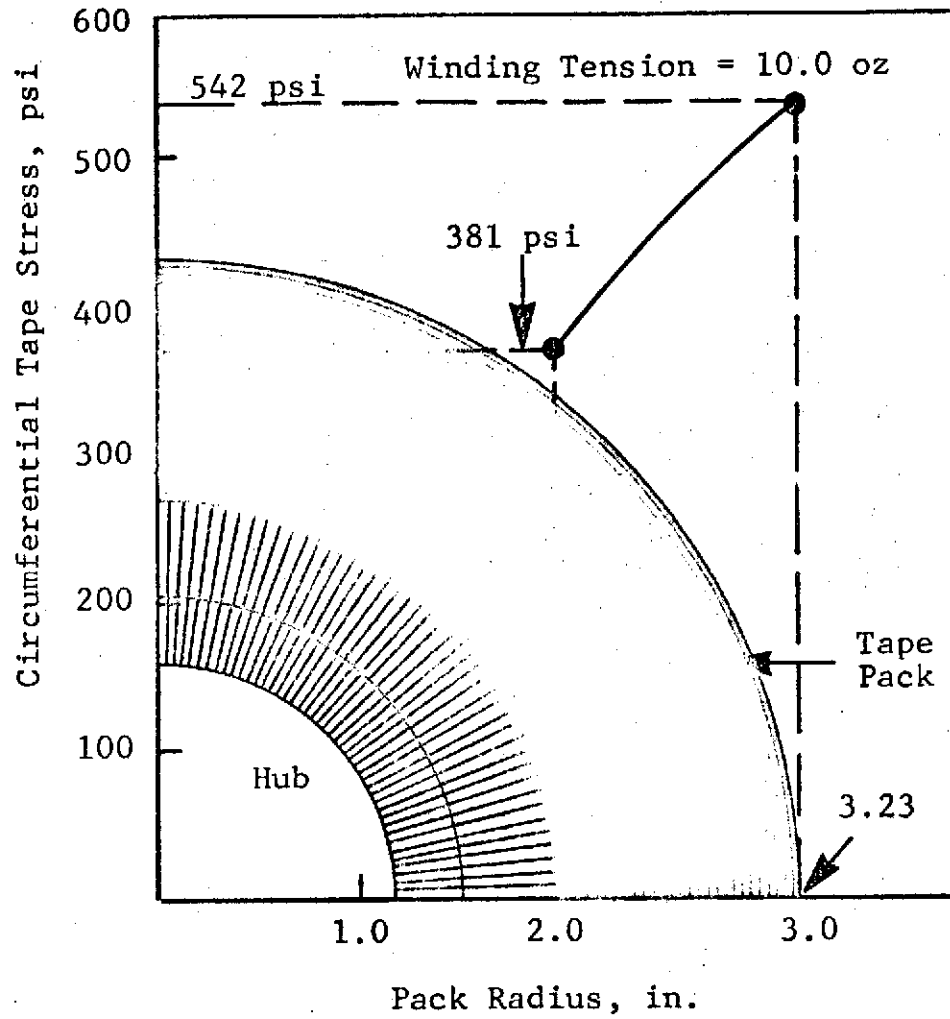


Figure 3.2 ACTUAL TAPE PACK STRESS DISTRIBUTION

### 3.1.2 Tape Stresses Over Capstans

Two capstans on either side of the head, and of rather large (1-1/4 in.) diameter have been selected. The larger diameter is desirable to minimize stress values especially since the oxide side of the tape is against one of the capstan surfaces, which is a slightly higher stress condition. The effects of tape tension, roller diameter, tape width, and surface contact width were examined. The calculated maximum tensile stresses occurring in the tape for the various conditions are shown in Table 3.1. For the selected roller, the maximum stress will be 1274 psi which is an extremely low tape stress conditions.

### 3.1.3 Capstan Wrap Angle

The present configuration utilizes two capstans of 1.25 inch diameter. The wrap angles have been selected at 165° and 180°. The adequacy of these wrap angles is established by calculating the tension ratio as shown in Figure 3.3. For an assumed tape to capstan friction coefficient of 0.8 a tension ratio greater than 10 to 1 exists. For an incoming tape tension of 8 oz., about 80 oz. would be required to cause tape slippage. Since the expected head tension will be from 8 to 12 oz., the wrap angles are sufficient to prevent slippage.

The capstan surfaces are cast and machined with a thin layer of conothane rubber. This material develops a friction coefficient with the tape of 0.8 or more.

### 3.1.4 Tape Stresses Over Crowned Idlers

The determination of tape stresses occurring over crowned rollers is complex. The distribution of stress that occurs over such rollers can be computed using the IITRI model (see Appendix C, Vol. III). As an example the longitudinal stresses occurring over a 2° double coned roller are shown in Figure 3.4. Without any rounding-off of the apex, the tape must bend laterally, i.e., across the width. Furthermore, the lateral bending radius will approach

Table 3.1

FEASIBILITY MODEL, FIVE YEAR RECORDER  
STRESSES OVER CYLINDRICAL CAPSTANS

<u>Oxide</u> <u>Out, I = 1</u> <u>In, I = 0</u>	<u>Roller</u> <u>Diameter</u> <u>(in.)</u>	<u>Tape</u> <u>Tension</u> <u>(oz)</u>	<u>Tape</u> <u>Width</u> <u>(in.)</u>	<u>Maximum</u> <u>Stress</u> <u>(psi)</u>	<u>Contact</u> <u>Width</u> <u>(in.)</u>
1	1.25	8.0	1.0	1143	1.0
0	1.25	8.0	1.0	1101	1.0
1	1.00	8.0	1.0	1296	1.0
1	1.50	8.0	1.0	1040	1.0
1	1.25	10.0	1.0	1274	1.0
1	1.25	12.0	1.0	1406	1.0
1	1.25	8.0	0.50	1671	1.0
1	1.25	8.0	0.75	1319	1.0

Tape Thickness = 0.00112 in.

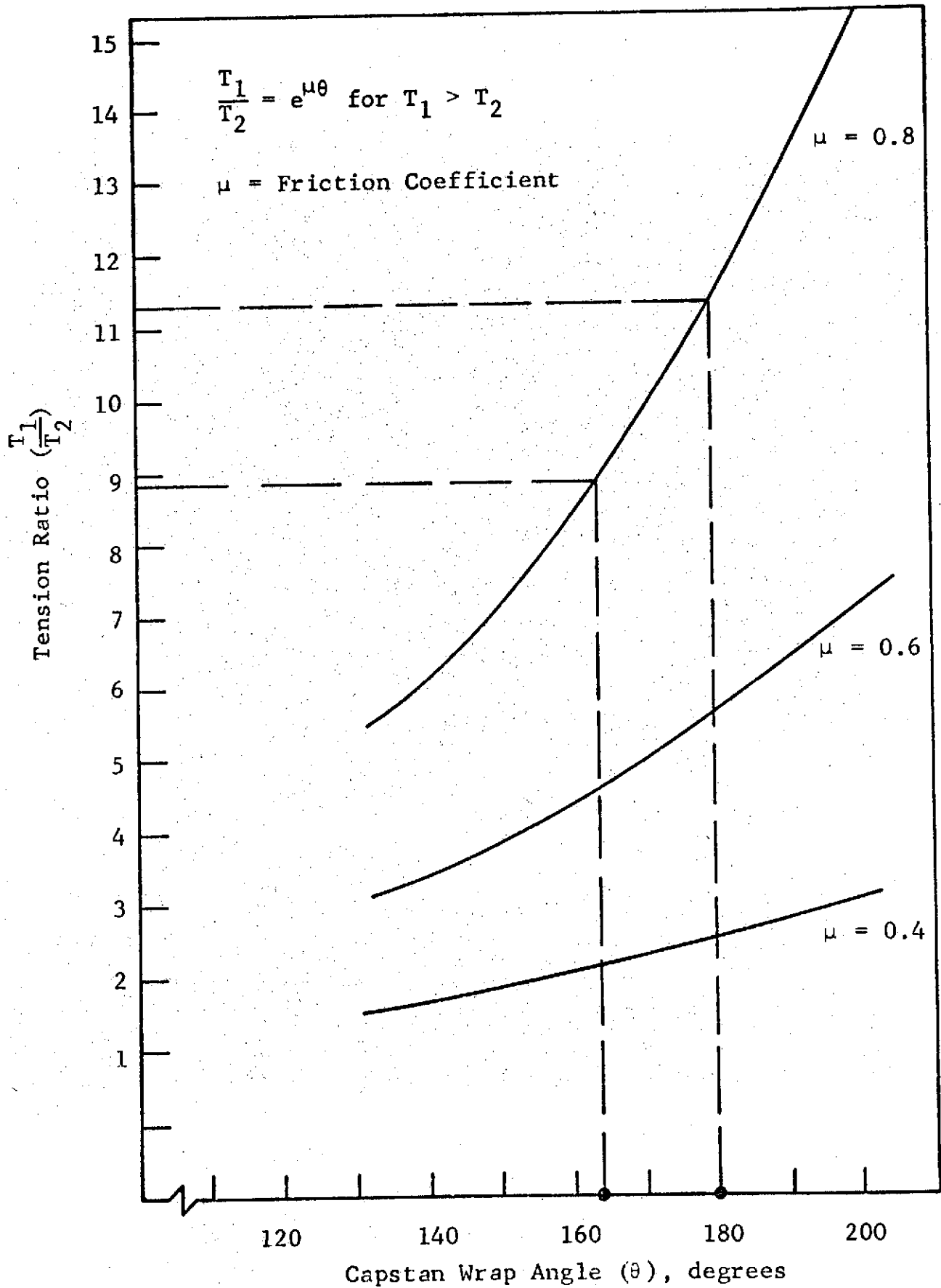
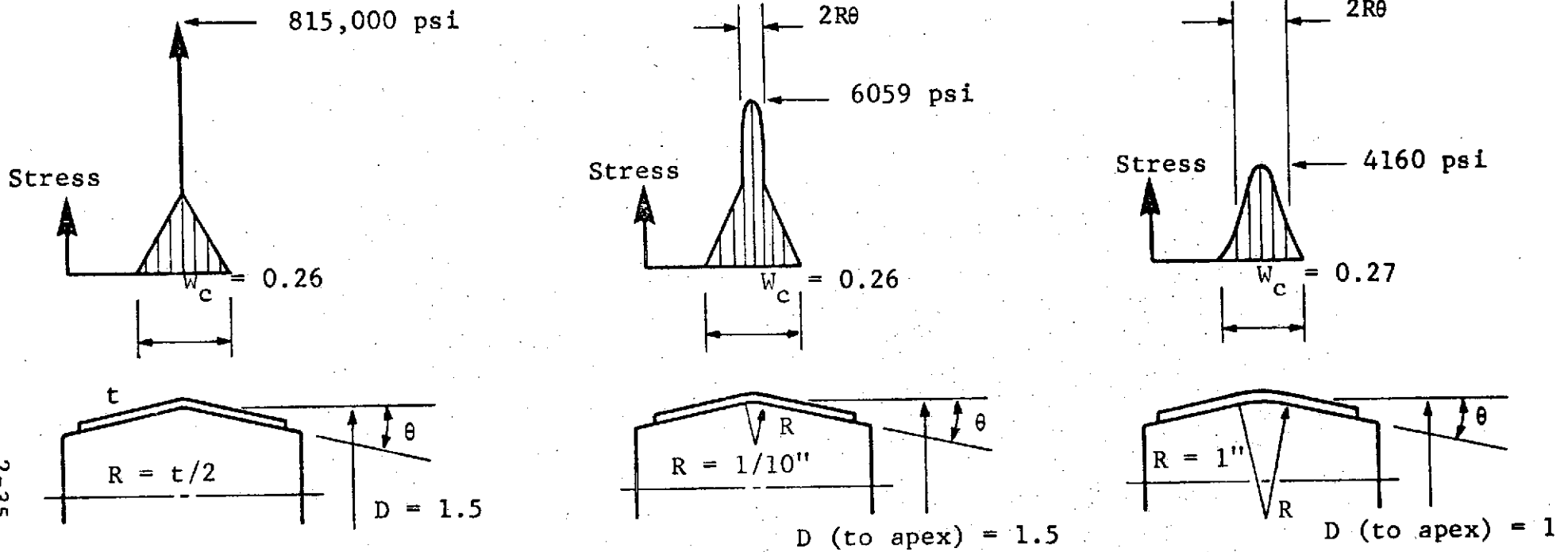


Figure 3.3 TENSION SLIP RATIO FOR CAPSTANS  
2-34



- T = tape tension, 8 oz
- t = tape thickness, 0.00112 in.
- D = roller diameter, 1.5 in.
- R = crown roller
- $\theta$  = cone angle,  $2^\circ$
- $w_c$  = contact width, in.

NOTE:  $R \geq \frac{D}{2}$  ( $R \geq D$ , preferred)

Figure 3.4 TAPE STRESS DISTRIBUTIONS OVER CROWNED ROLLERS

half the tape thickness and give rise to extremely high stresses. Continued operation over a sharp apex would quickly damage the tape.

The second distribution given in Figure 3.4 shows the rapid decrease in peak stress due to rounding-off of the apex. Note that the contact width is about 1/4 inch. This contact width is developed on a one inch wide tape under an 8 oz. tension. Furthermore, it should be noted that the stress distribution and stress magnitude is mainly dependent upon the contact width and not the tape width, that is, a 1/4, 1/2, or 1 inch wide tape would all develop the same stress distribution and magnitude.

Rounding-off of the apex angle, converts a portion of the double cone roller into a spherically crowned roller. The width of the round-off portion is given by;

$$\text{Round-Off Width} = 2R\theta$$

where  $R$  is the radius, and  $\theta$  is the cone angle in radians. For a  $2^\circ$  cone angle and a round-off radius of 0.1 inches, the round-off width is 0.007 inches. Since this width is small compared to the tape contact width (0.26 inches), the roller operates as a double cone.

Increasing the round-off radius will eventually convert the double-coned roller into a spherically crowned roller. This transition will occur when the round-off width equals or exceeds the contact width. For the  $2^\circ$  coned roller considered here, this transition will occur when the round-off radius is about 3.5 inches.

The effects of rounding-off the cone apex is shown in Figure 3.5. Of particular importance is the decrease in peak stress with increased crown (round-off) radius. It is recommended that the crown radius be at least equal to or greater than the roller radius, that is, transverse tape bending should not exceed longitudinal tape bending. Table 3.2 summarizes the calculations by

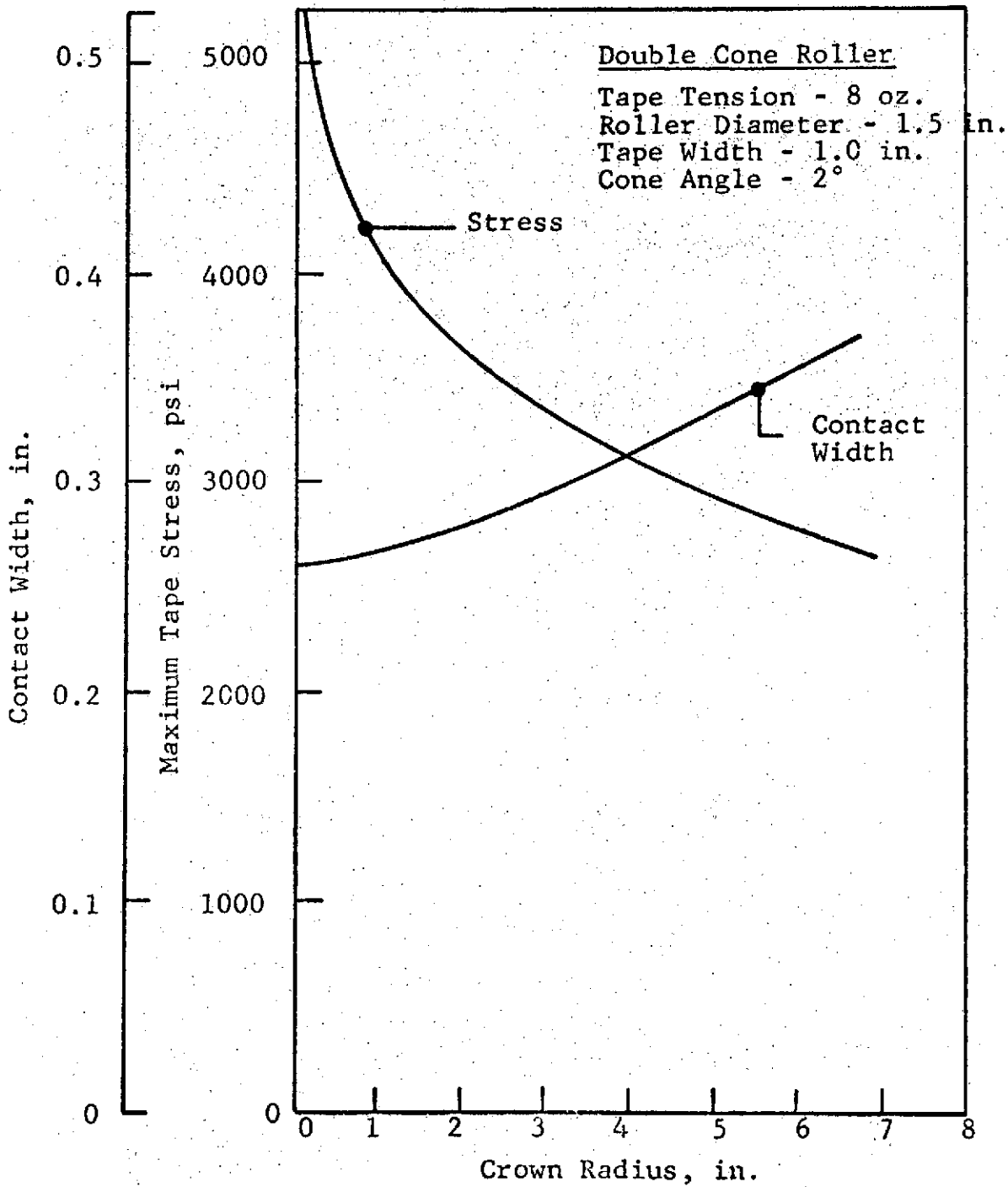


Figure 3.5 EFFECTS OF ROUND-OFF



Table 3.2

DOUBLE CONED IDLER STRESSES

<u>Roller Diameter (in.)</u>	<u>Tape Tension (oz)</u>	<u>Tape Width (in.)</u>	<u>Crown Radius (in.)</u>	<u>Cone Angle (deg)</u>	<u>Maximum Stress (psi)</u>	<u>Contact Width (in.)</u>
1.5	8.0	1.0	0.5	2.0	4554	0.26
1.5	10.0	1.0	0.5	2.0	5027	0.29
1.5	12.0	1.0	0.5	2.0	5454	0.32
1.5	8.0	0.50	0.5	2.0	4554	0.26
1.5	8.0	0.75	0.5	2.0	4554	0.26
1.5	8.0	1.0	0.5	1.0	3569	0.37
1.5	8.0	1.0	0.5	3.0	5159	0.22
1.5	8.0	1.0	0.1	2.0	6059	0.26
1.5	8.0	1.0	1.0	2.0	4160	0.27
1.5	8.0	1.0	3.5	2.0	3211	0.30
1.5	8.0	1.0	3.0	2.0	3400	0.29

Mylar Thickness = 0.00092

Oxide Thickness = 0.00020

Elastic Modulus for Mylar = 650,000 psi

Poisson's Ratio for Mylar = 0.45

Oxide away from Roller Surface

illustrating the maximum longitudinal tape stress by a double coned roller, where, the effect of a change in cone angle, tape tension, tape width, and crown radius is tabulated.

The last line in Table 3.2 shows the crowned idler selected for the 5-year transport. This roller has a 1.5 inch diameter, a 2° cone angle and a 3 inch round-off radius. This roller gives excellent guidance while inducing a tape stress of only 3400 psi.

### 3.1.5 Head Stresses and Pressure

The storage and retrieval of information using a satellite recorder requires intimate contact between the tape and the record head. Therefore, it is first necessary to establish the required head pressure.

Previous head/tape interface studies conducted by IITRI, reveal the head pressure should be about 80 oz./inch<sup>2</sup>. This pressure can be achieved for a one inch tape width using a head radius of 1/8 inch and a tape tension of 10 oz. as shown in Figure 3.6. The pressure relationship shown in the figure is an approximation which assumes the effect of wrap angle on pressure is negligible.

The stresses induced in the tape as it passes over the heads are calculated from the same program used for the capstans. In other words, the head behaves as a straight roller with a small radius equal to the head radius.

The maximum tensile stress occurring in the mylar was calculated for a one inch wide tape running under different tensions over various radii heads. The results are shown in Figure 3.7. Thus, a head radius of 1/8 inch with a tape tension between 8 to 10 oz. will produce stresses of 3500 psi and 3730 psi respectively. These stresses are slightly above the established guideline of 3500 psi maximum stress, but should be adequate to insure a five year life.

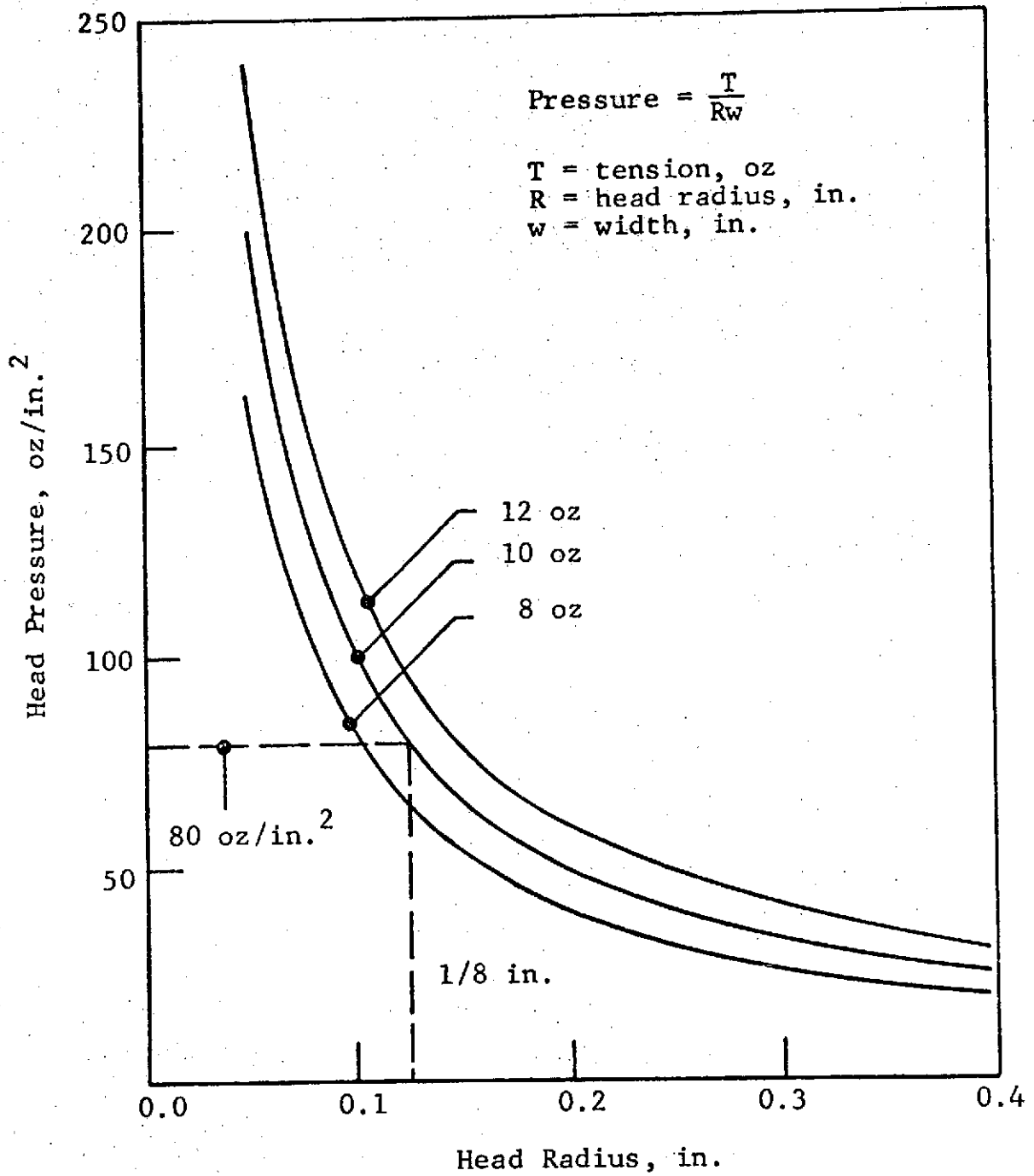


Figure 3.6 HEAD PRESSURE STUDY

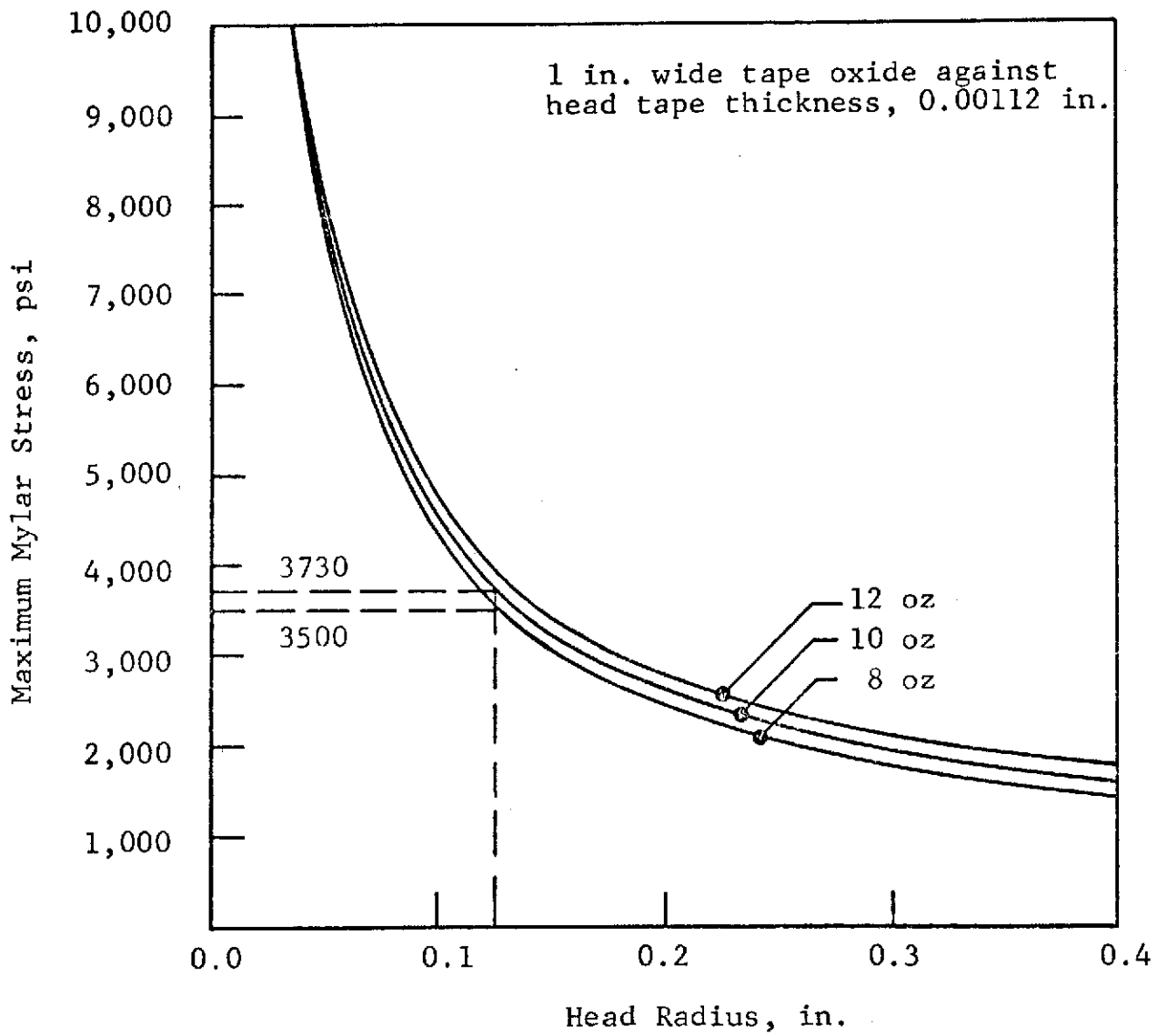


Figure 3.7 HEAD STRESS STUDY

### 3.1.6 Free Length Tape Stresses

The free lengths of tape between the rotating elements are under tension loads only. Therefore the tape stresses are tensile. Furthermore the tape is basically a composite of mylar and oxide layers with differing moduli of elasticity. Hence, the tensile stress developed in each layer is given by:

$$S_o = \frac{T}{w \left[ t_o + t_m \frac{E_m}{E_o} \right]}$$

and

$$S_m = \frac{T}{w \left[ t_m + t_o \frac{E_o}{E_m} \right]}$$

where

$S_o$  = oxide tensile stress, psi

$S_m$  = mylar tensile stress, psi

$T$  = total tape tension, lb.

$w$  = tape width, in.

$t_o$  = oxide thickness, in.

$t_m$  = mylar thickness, in.

$E_o$  = oxide modulus, psi

$E_m$  = mylar modulus, psi

Evaluating these expressions for,

$E_m = 650,000$  psi

$E_o = 100,000$  psi

$t_m = 0.00092$

$t_o = 0.00020$  in.

$w = 1.0$  in.

$T = 0.5$  lb. (8 oz.)

IIT RESEARCH INSTITUTE

yields stress values in the mylar and oxide layers of

$$S_m = 526 \text{ psi}$$

$$S_o = 81 \text{ psi}$$

### 3.1.7 Tape Stress Summary

A complete stress profile of a tape element, as it passes from one reel to the next, is shown in Figure 3.8. It is seen that only the crowned idlers and the recording head induce significant tape stresses. Therefore, the tape will be subjected to three significant stress cycles per record pass. Furthermore, since a five year life represents approximately 25,000 recordings (50,000 tape cycles), the tape will be subjected to 150,000 stress cycles during its life. The magnitude of these stress cycles is about 3500 psi which is within the long life guidelines.

### 3.2 Guidance Analysis

Lateral tape position errors are introduced at the recording head due to machining and assembly tolerance errors. Although such errors can never be completely eliminated, they can be attenuated by crowned guidance idlers and held to acceptable limits of lateral tape movement at the head.

In order to predict the guiding action of crowned idlers analytically, a mathematical simulation suited for digital computer execution was developed. The model, described in Appendix A, considers the action of a crowned idler guiding a piece of tape as similar to that of a screw. As the tape advances, the idler attempts to screw the tape over to an equilibrium position where lateral forces within the tape are balanced on either side of the idler. In the analysis it is assumed that frictional forces between the idler and the tape are sufficient to prevent any gross relative motion.

The guidance capabilities of a double coned idler, as shown in Figure 3.9, were determined using the mathematical model described above. Parameters used in the analysis are shown in Table 3.3.

Tape Stress, psi

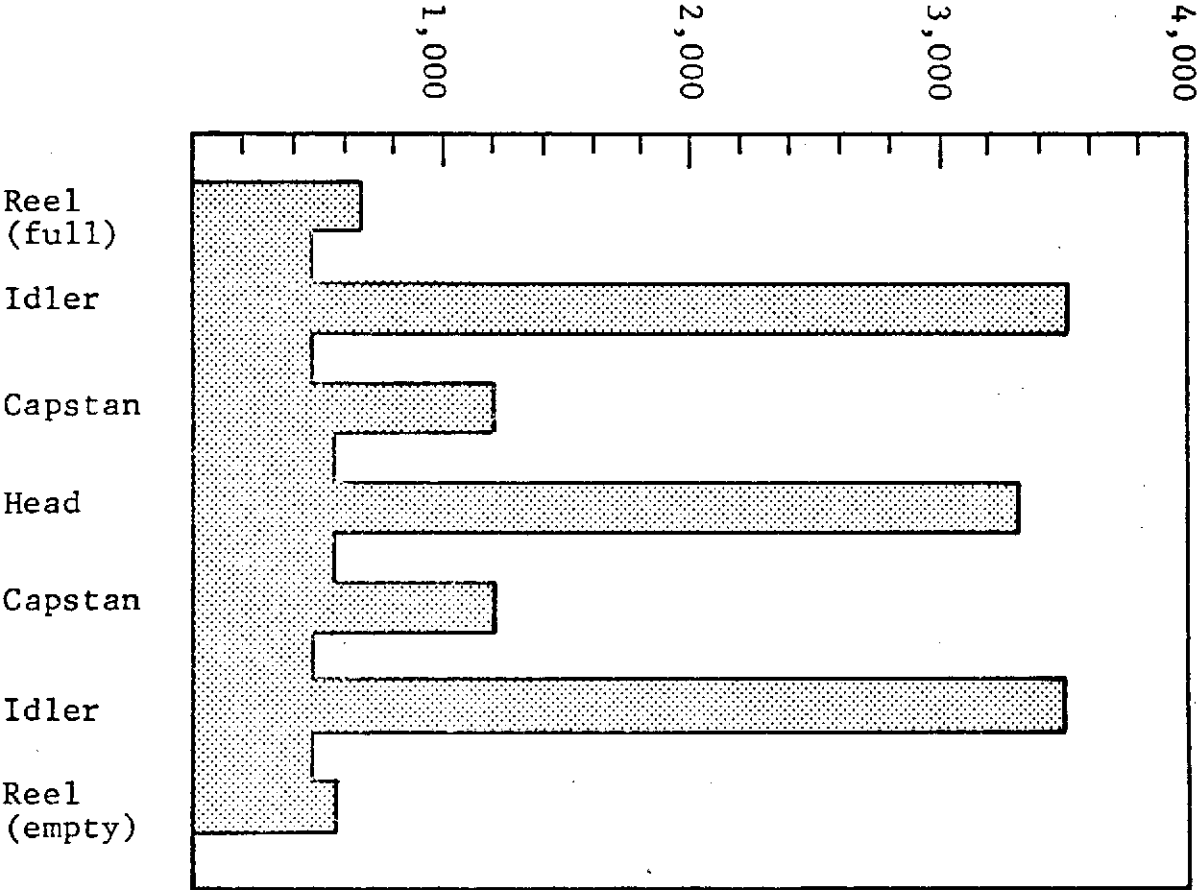


Figure 3.8 TAPE STRESS PROFILE

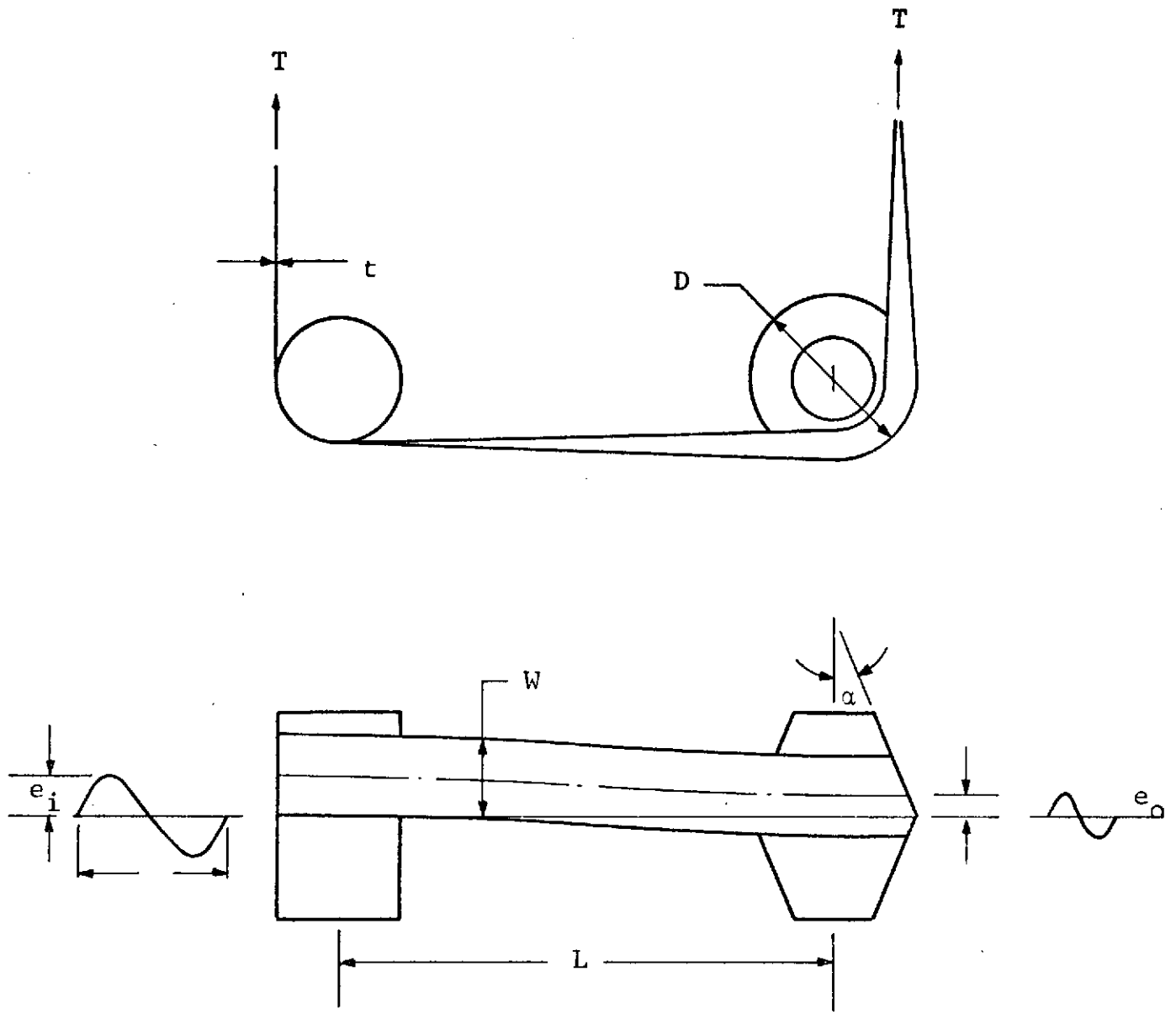


Figure 3.9 DOUBLE-CONED IDLER GUIDANCE MODEL



Table 3.3

## PARAMETER VALUES USED IN GUIDANCE ANALYSIS

<u>Parameter</u>	<u>Value</u>
Tension, T	10 oz.
Tape width, W	1.0 in.
Idler diameter, D	1.5 in.
Cone angle, $\alpha$	2.0 deg
Input amplitude, $e_i$	0.020 in.
Input wavelength, $\lambda$	4.0 in.
Tape thickness, t	0.00112 in.

The tape leaving the cylindrical roller was given a harmonic perturbation in the lateral direction simulating axial play in the roller. The amplitude of this tape disturbance after leaving the coned idler was determined by the simulation model. Attenuations were calculated using equation (1) below:

$$A = \left(1 - \frac{e_o}{e_i}\right) \times 100 \quad (1)$$

where:

$A$  = idler attenuation, percent

$e_i$  = input amplitude at cylindrical roller, in.

$e_o$  = output amplitude at coned idler, in.

Computed values are shown in Table 3.4 for the forward and reverse directions of tape travel with full and empty reels.

Using the attenuation of the individual coned idlers given in Table 3.4, a system attenuation was computed to establish how tape disturbances would diminish with multiple passes over coned idlers. System attenuations, computed from equation (2) are shown in Table 3.5.

$$A_{\text{sys}} = 100 - (1 - A_1) (1 - A_2) \dots (1 - A_n) \quad (2)$$

where:

$A_{\text{sys}}$  = system attenuation, percent

$A_i$  = attenuation of idlers in tape path, percent  
( $i = 1, 2, \dots, n$ )

### 3.3 Natural and Induced Frequencies

The calculation of undamped system natural frequencies are useful in system design since coincidence of induced disturbance frequencies can cause resonance. The result is performance and/or life degradation. Therefore, the natural frequencies are calculated for the reel tape system.

Table 3.4

## CALCULATED ATTENUATION VALUES FOR INDIVIDUAL IDLERS

<u>Direction of Travel</u>	<u>Attenuation, %</u>
<u>Forward</u>	
LH reel (full) - idler No. 1	48.20
LH reel (empty)- idler No. 1	47.85
Capstan No. 2 - idler No. 2	61.58
<u>Reverse</u>	
RH reel (empty)- idler No. 2	46.39
RH reel (full) - idler No. 2	41.24
Capstan No. 1 - idler No. 1	47.49

Table 3.5

## SYSTEM ATTENUATION VALUES

<u>Direction of Travel</u>	<u>System Attenuation, %</u>
Record (full LH reel)	80.10
Record (empty LH reel)	79.96
Play (empty RH reel)	71.85
Play (full LH reel)	69.15

The frequencies of importance arise in two ways. The first is the result of the reels, capstans and idlers behaving as rigid inertial elements connected by elastic tape lengths. Thus, the system has certain built-in modes of vibration and associated frequencies which must not be excited.

The IITRI developed computer program was used to calculate the first four mode frequencies. This program idealizes the reel/capstan/idler/tape system as a lumped mass, linear spring, torsional system. Natural frequencies are found using the Holzer method. These computed system frequencies are shown in Figure 3.10.

The second way in which natural frequencies arise has to do with the unsupported tape lengths adjacent to the head. These tape lengths exhibit both lateral (strumming) and longitudinal natural frequencies.

The first mode longitudinal frequency and the first three mode strumming frequencies are also shown in Figure 3.10. These values were calculated using a centrally mounted head, i.e., equal tape length on either side of the head.

Induced excitation frequencies, capable of exciting the above natural frequencies, may be generated by any of the rotating elements. In particular, eccentricities of the reels, capstans and idlers generate the primary excitation frequencies. These frequencies are dependent upon the rotational speeds of the elements. In addition, the rotating bearing balls will generate certain higher frequencies.

Those induced frequencies above 10 Hz are shown in Figure 3.10 for easy comparison with the natural frequencies. The only potential resonance problem could be the excitation of the first mode system frequency at 72 ips (play mode).

### 3.4 Kinetic Properties

The kinetic properties of the tape reeling system have been computed and are presented in this section. These properties include the mass moment of inertia of the reels, the reeling

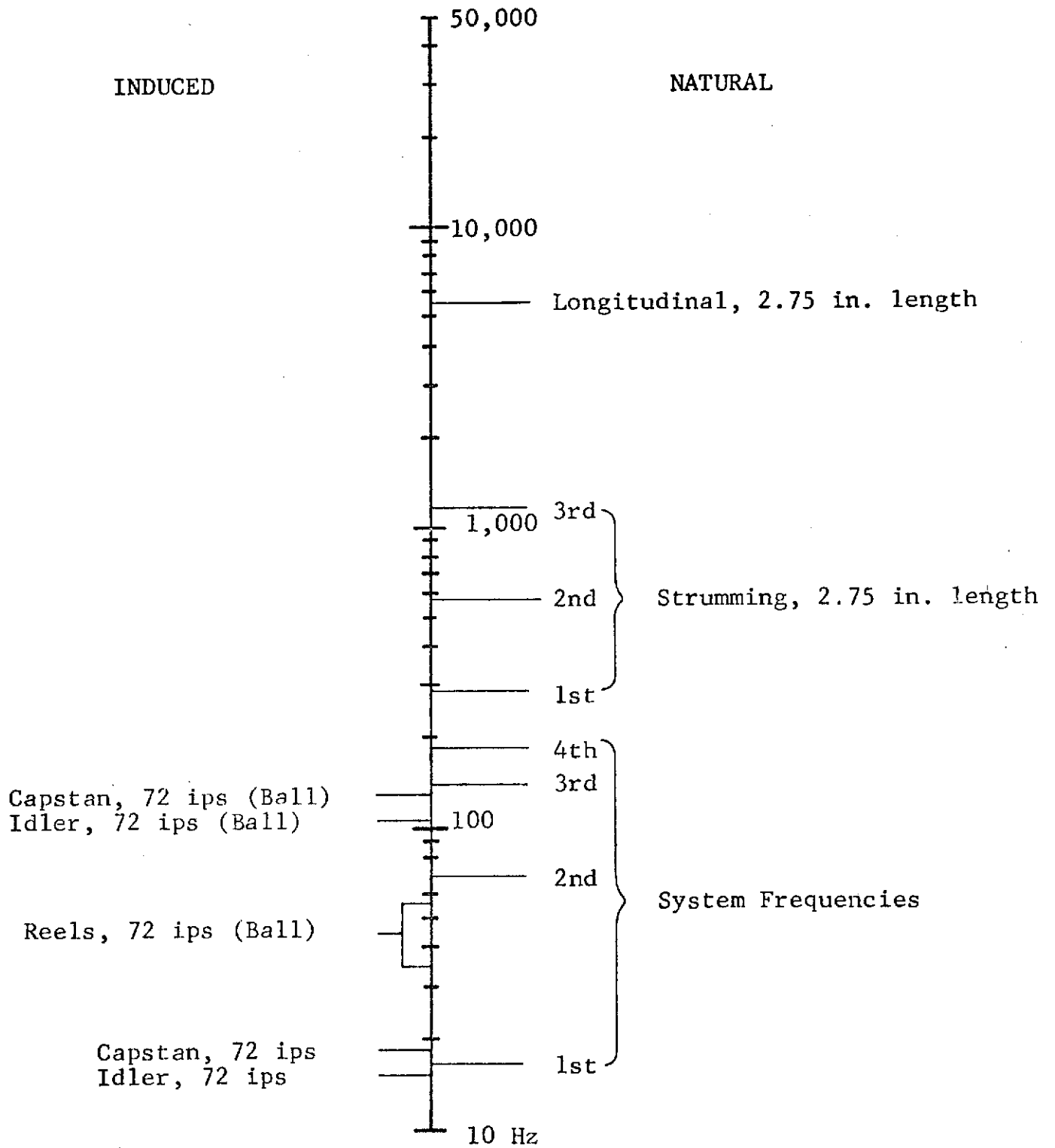


Figure 3.10 SYSTEM NATURAL AND INDUCED FREQUENCIES ABOVE 10 Hz

torques, the angular velocities of the reels, the power required to drive the reels, and the angular momentum developed.

The recorder has been designed to operate with 1500 ft. of one inch wide magnetic tape. The coplanar reels (see Figure 3.1) have a hub diameter of 4 inches. The radius of the tape pack as a function of tape length is shown in Figure 3.11. At the midtape position, the pack radius is approximately 2.68 inches. Allowing for clearance and additional tape for lead-in, the reel center distance is set at 5.562 inches.

The torque developed by an 8 ounce tape tension is shown in Figure 3.12. The actual or true torque developed will differ slightly from the values given in the figure since the angular acceleration and frictional effects have been omitted. These effects, however, account for variations of less than  $\pm 0.1$  percent.

The angular velocity or speed of a reel during the record and play modes is shown in Figures 3.13 & 3.14 respectively. A 1.614 to 1 speed ratio is developed as a result of the changing pack diameter.

The moment of inertia of a single reel and tape pack is given in Figure 3.15. The inertia of an empty reel is 0.0108 in.-lb.-sec.<sup>2</sup> and increases to 0.0586 in.-lb.-sec.<sup>2</sup> with the addition of 1500 ft. of tape. The kinetic energy developed by a reel and tape pack during high speed operation (play mode) is shown in Figure 3.16.

The 5 year transport maintains a constant tape tension through the use of two reel motors. The motors are used alternately as a driver and a brake. Consequently, each reel motor consumes power during both record and play modes. The total power required by the reels during record is given by:

$$P = 2(0.113 Fv)$$

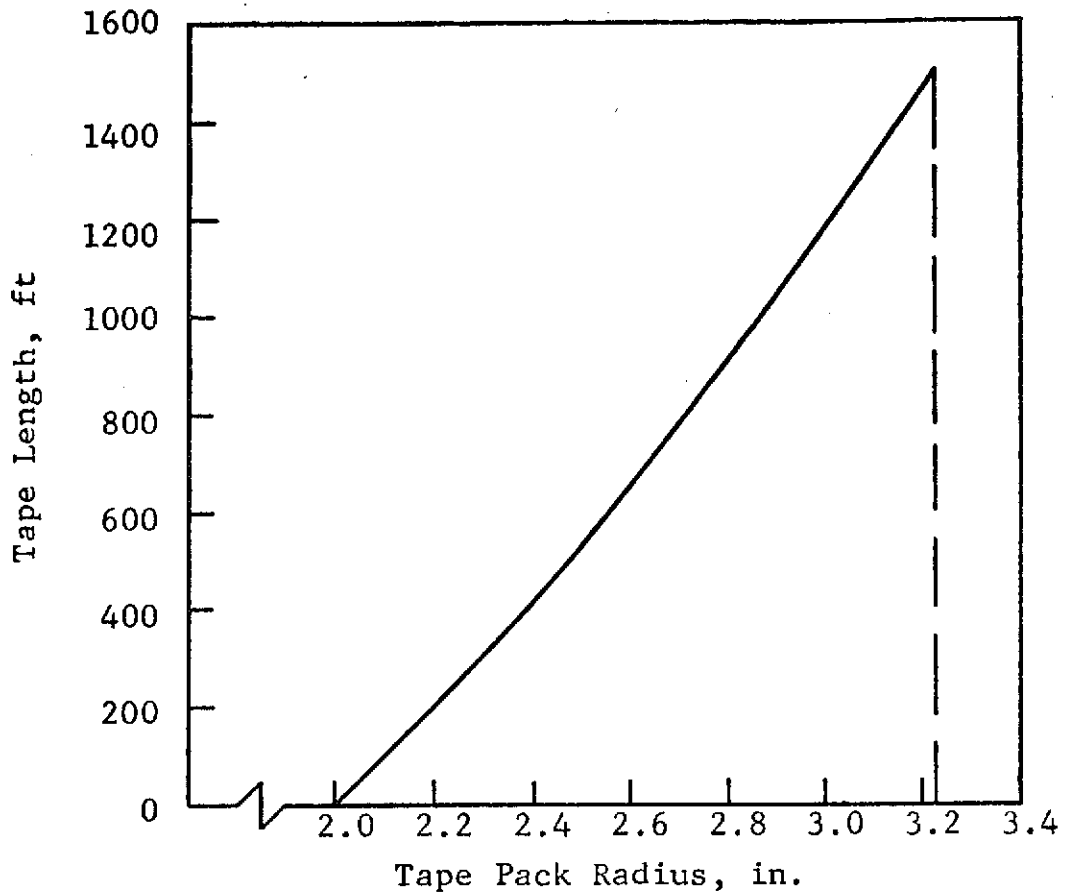


Figure 3.11 TAPE PACK RADIUS VERSUS LENGTH

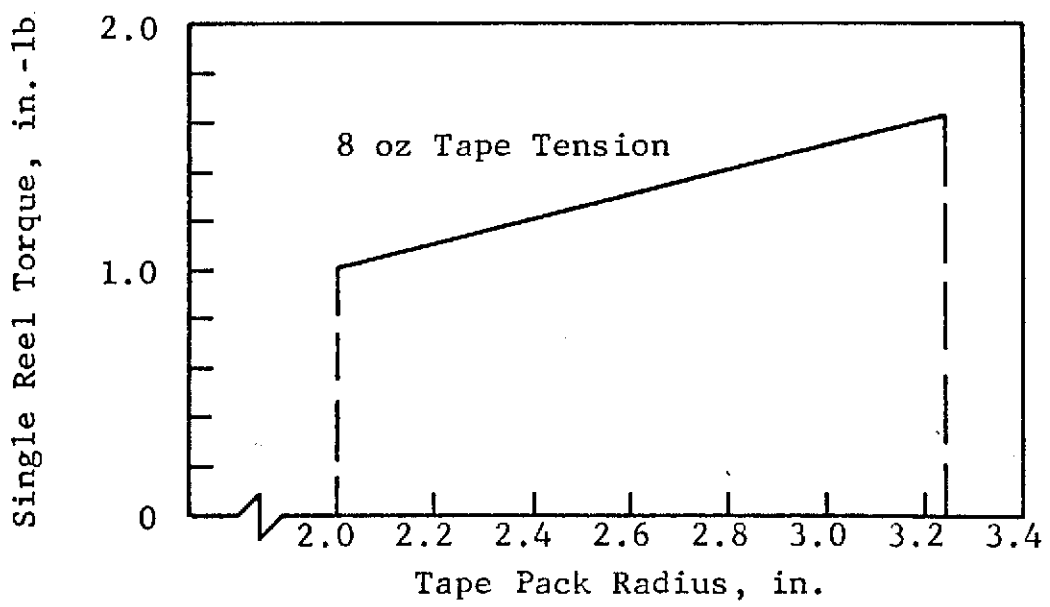


Figure 3.12 TORQUE DEVELOPED BY TAPE TENSION

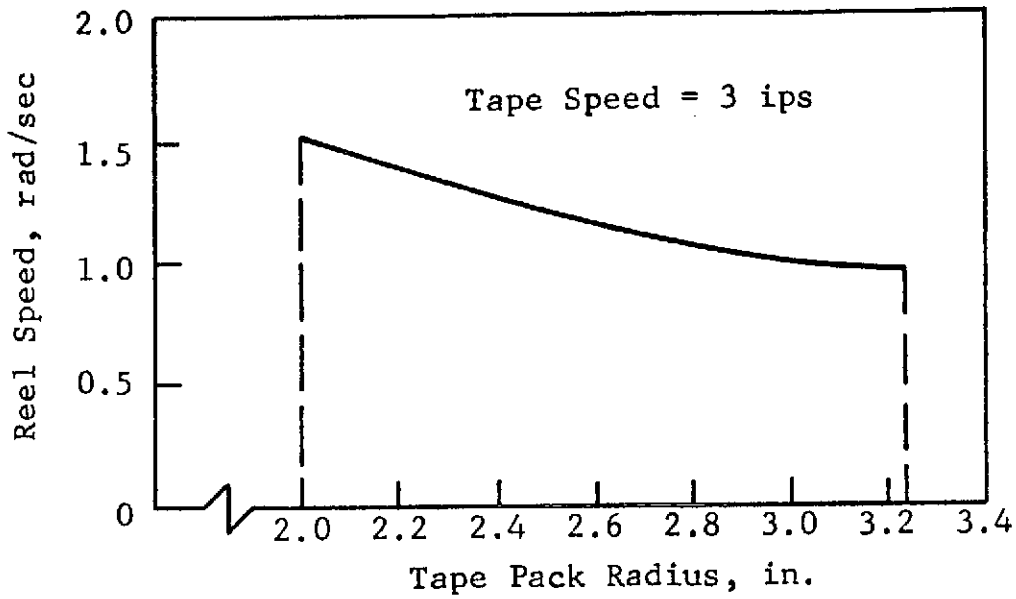


Figure 3.13 REEL SPEED DURING RECORD MODE (3 ips)

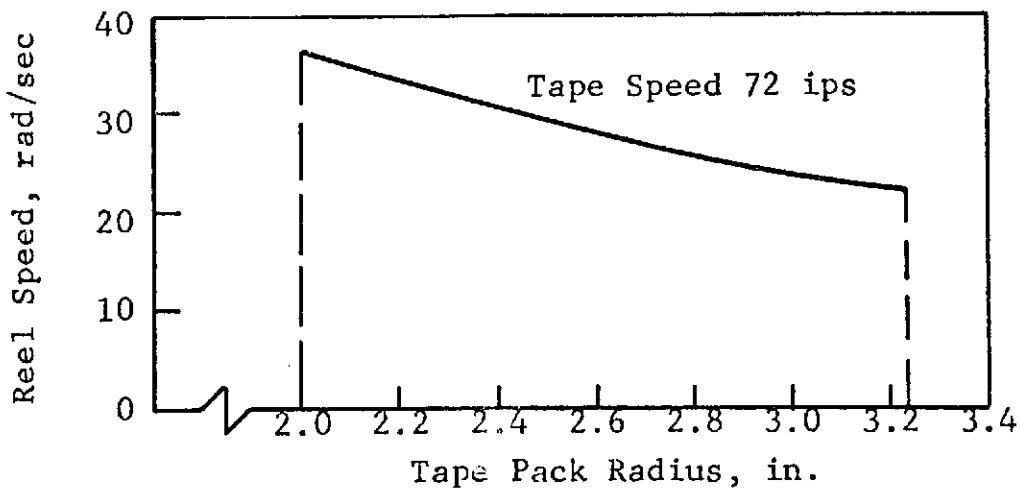


Figure 3.14 REEL SPEED DURING PLAY MODE (72 ips)



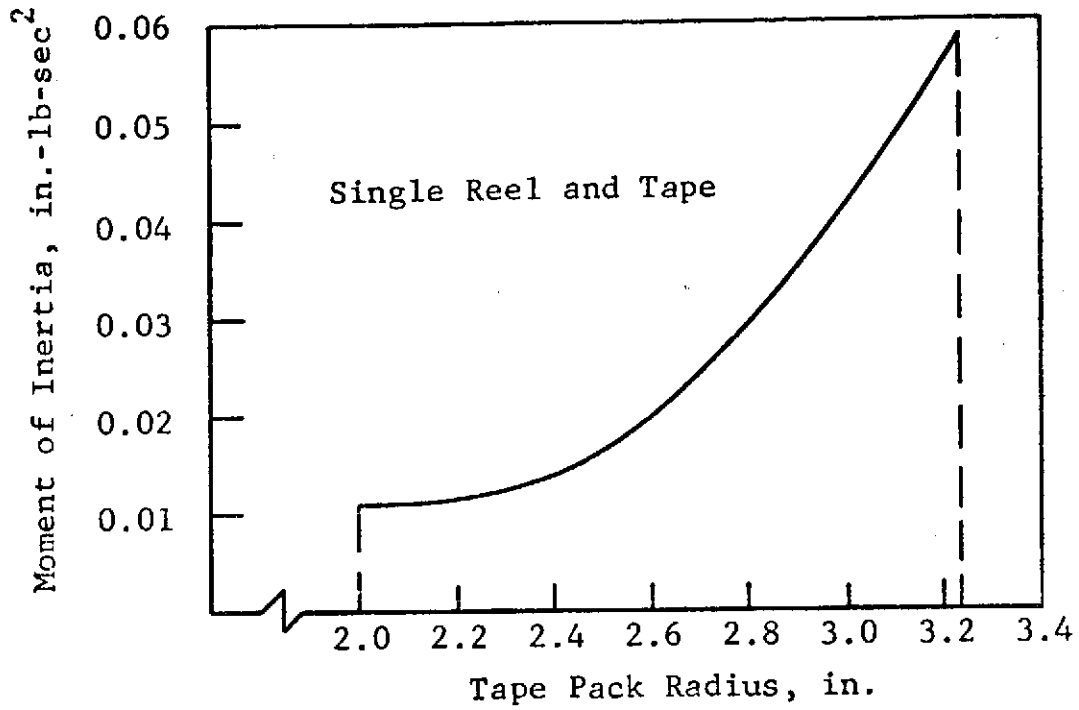


Figure 3.15 TAPE PLUS REEL INERTIA

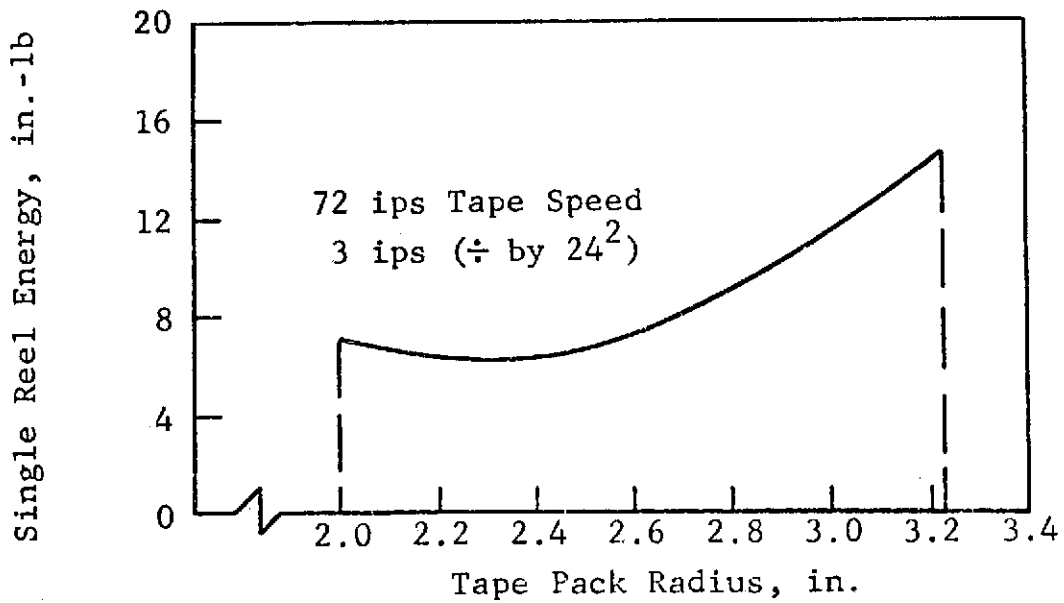


Figure 3.16 TAPE PLUS REEL KINETIC ENERGY

where

P = total reel power, watts

F = tape tension, lb.

v = tape speed, ips

0.113 = conversion factor

For an 8 ounce (1/2 lb.) tape tension and a record speed of 3 ips, the total power consumed by the two reel motors is:

$$P = 2(0.113) (1/2) (3) = 0.339 \text{ watts}$$

Similarly the power consumed during the play mode with a tape speed of 72 ips is:

$$P = 2(0.113) (1/2) (72) = 8.136 \text{ watts}$$

### 3.5 Bearings

The IITRI transport uses precision anti-friction ball bearings in all of the rotating modules. A highly reliable bearing system was obtained by utilizing conservative design procedures in the selection. In addition, meticulous cleanliness procedures and cautious assembly practice was maintained during fabrication. Furthermore, a design was developed for each module that allows an accurate bearing preload to be established and maintained.

The specifications for the selected bearings are given in Table 3.6. All the bearings are deep-grooved with phenolic retainers. Andoc-C grease was selected as the best available lubricant.

In recent years a better understanding of rolling-element bearing design, materials processing, and manufacturing techniques has permitted a general improvement in bearing performance. This is witnessed in higher bearing reliability and longer life for a given application. In addition, the quantifying of environmental

TABLE 3.6  
BEARING SPECIFICATIONS

	<u>IDLERS AND CAPSTANS</u>	<u>REELS</u>
Manufacturer	Barden	Barden
Bearing Number	SFR6SS	A538T
Code Number	4	4
Type	Flanged, Deep Grooved	Large Bore, Deep Grooved
O.D.	0.875 in.	1.0625 in.
I.D.	0.375 in.	0.625 in.
Width	0.2812 in.	0.250 in.
Number of Balls	7	10
Ball Diameter	5/32 in.	1/8 in.
Contact Angle	7°	15°
Retainer	One-Piece Phenolic	Two-Piece Phenolic
Pre-Load, lbs.	1 ± 1/4	1-1/2 ± 1/4
Lubricant	Andoc-C Grease	Andoc-C Grease Vacuum Impregnated Retainer

factors permits much better estimates of expected bearing life. One such life prediction method,<sup>(1)</sup> and the one selected by IITRI in assessing the 5-year transport bearings, was compiled by the Rolling-Elements Committee of the American Society of Mechanical Engineers (ASME). This method assumes that various environmental design factors, at least for first-order effects, are multiplicative. As a result, the expected bearing life  $L_A$  can be related to the manufacturer rated life ( $L_{10}$ ) by the following expression:

$$L_A = (D) (E) (F) (G) (H) L_{10}$$

or

$$L_A = (D) (E) (F) (G) (H) \left[ \frac{C}{P} \right]^n$$

where

C = basic dynamic radial load rating, lb.

P = equivalent radial load, lb.

n = load-life exponent (n = 3 for ball bearings)

D...H = life adjustment factors.

The basic dynamic radial load rating is taken from the manufacturer's (Barden) catalog.<sup>(2)</sup> These values are given in Table 3.7. In addition, the equivalent radial load P, is computed from the expression,

$$P = XP_r + YP_a$$

where:

$P_r$  = radial load, lb.

$P_a$  = axial load, lb.

---

(1) "Life Adjustment Factors for Ball and Roller Bearings", ASME Engineering Design Guide, 1971, New York.

(2) "Engineering Catalog G-3", The Barden Corporation, Danbury, Connecticut.

TABLE 3.7  
BEARING LIFE DATA

<u>Bearing</u>	<u>Capstan Bearing # SFR6SS</u>	<u>Idler Bearing # SFR6SS</u>	<u>Reel Bearing # A538 T</u>
RPM at 3 ips tape speed	45.83	38.19	8.8 full 14.3 empty
RPM at 72 ips tape speed	1100	916	213 full 344 empty
Revolutions per 1500 ft. of tape	4583	3819	1100
Revolutions per 50,000 passes (5 years)	$2.29 \times 10^8$	$1.91 \times 10^8$	$0.55 \times 10^8$
Radial load $P_r$ , oz.	20	18	10
Axial load $P_a$ , oz.	2	3	50
Contact Angle, deg	7	7	15
Radial load factor, X	0.52	0.52	0.44
Thrust load factor, Y	3.5	3.5	1.7
Equivalent radial load, P, lb	1.087	1.137	5.595
Basic dynamic radial load rating, C, lb	357	357	495
Expected life, $L_A$ , hrs	$19.6 \times 10^6$	$17.4 \times 10^6$	$0.4 \times 10^6$

---

Note: 5 years =  $4.38 \times 10^4$  hrs.

X = radial load factor

Y = axial load factor

The computed values for these factors are given in Table 3.7 for each of the three module bearings. The values for the life adjustment factors are taken from the figures and tables given in Reference 1. These values are:

D = 0.2 (material factor)

E = 1.0 (processing variable)

F = 0.4 (lubrication factor)

G = 0.7 (speed effect)

H = 0.2 (misalignment factor)

The cumulative product of these factors is 0.0112 so the expected bearing life equation is then given by:

$$L_A = 0.0112 \left[ \frac{C}{P} \right]^3$$

Evaluating this equation for each of the three bearings yields the life in hours as shown at the bottom of Table 3.7. These values are substantially larger than the required 5-years (43,800 hours) of continuous operation.

### 3.6 System Response

A response calculation yields a quantitative analysis of tape transport mechanical performance which is preferable to the qualitative measure of the natural frequency calculation. Using the computer program discussed in Appendix E, the transport tape response for inherent system excitations was computed. Excitations from component eccentricities were applied to the transport dynamic simulation model. Machining run-out errors manifest themselves as a once-per-revolution torque pulsation phenomena. In this section, the response calculation, shown for the IITRI Five-Year High Reliability Tape Transport, will be compared to experimental results.

Torque excitations are entered directly in the simulation program while displacement (eccentricities) must be related to excitation torques through the tape constants. The mathematical expressions for torque excitation as a function of tape constants, machining eccentricity and idler radius is derived with the aid of Figure 3.17. Equations (1) through (4) are derived for idler angular positions - 0, 90, 180, 270, and 360, assuming the tension is equal across the idler.

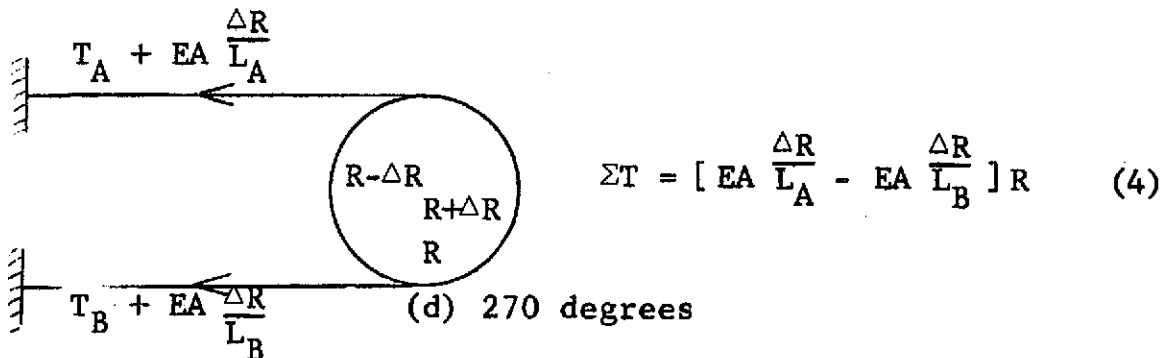
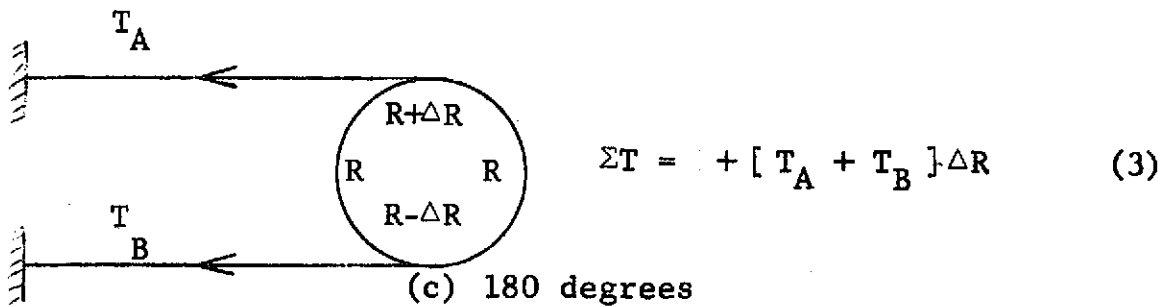
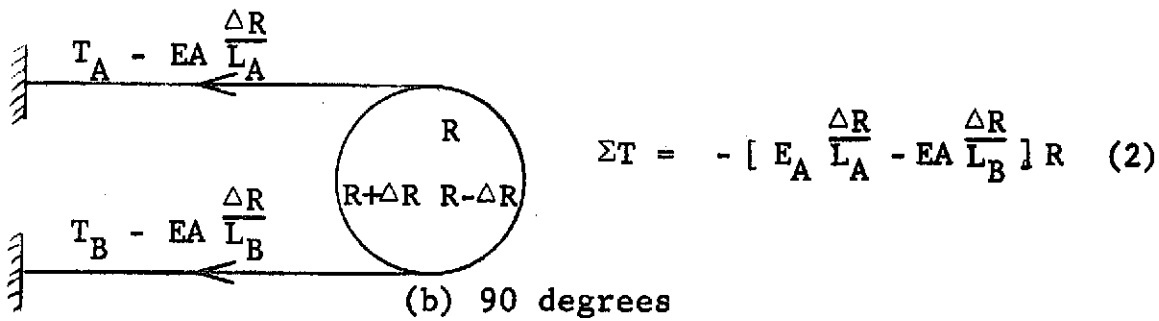
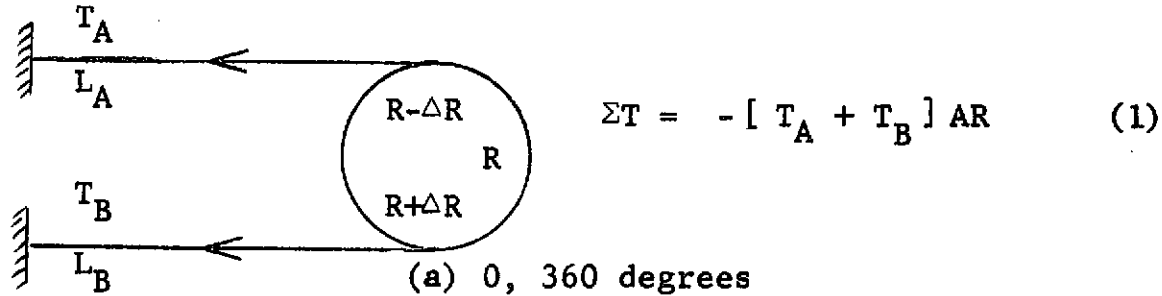


Fig. 3.17 The Relationship Between Eccentricity and Torque Excitation Magnitude

These four equations can be combined to obtain equation (5) which represents the mathematical relationship between eccentricity and exciting torque.

$$\tau = a \sin \omega t + b \cos \omega t \quad (5)$$

where  $\tau$  = torque excitation  
 $\omega$  = idler rotational frequency  
 $t$  = time  
 $a = REA\Delta R \left| \left( \frac{1}{L_A} - \frac{1}{L_B} \right) \right|$   
 $b = 2T R$   
 $T$  = tape tension  
 $\Delta R$  = eccentricity  
 $E$  = tape modulus of elasticity  
 $L_n$  = tape lengths  
 $A$  = tape cross-sectional area  
 $R$  = idler radius

The torque excitation for the Five-Year Tape Transport was calculated using the eccentricities and physical parameters shown in Table 3.8.

Table 3.9 shows the calculated response of the tape at the head for actual component run-out error for tape speeds of 3 ips and 60 ips. The response at the head due to 46x speed ripple torque when recording at 7.5 ips and 60 ips is also shown in Table 3.9. The response is shown in terms of instantaneous absolute displacement and flutter (rms velocity).



Table 3.8  
Physical Parameters For Tape Response Computation

Component (Eccentricity, in)	Tape Modulus (psi)	Tape Area (in <sup>2</sup> )	Tape Tension (oz)	Radius (in)	Tape Length Input (in)	Tape Length Output (in)	Excitation Constant (In-Lbs)	Excitation Constants (In-Lbs)	Excitation Freq. (Rad/Sec)
Crowned Idler (Left) (.00008)	500,000	.00112	12	.75	5.4	5.4	$4.6 \times 10^{-5}$	$8 \times 10^{-5}$	4.0 8.0
Capstan (Left) (.00028)			12	.625	5.4	2.3	$2.2 \times 10^{-2}$	$2.8 \times 10^{-4}$	4.8 96
Capstan (Right) (.00012)			12	.625	7.5	2.3	$1.1 \times 10^{-2}$	$1.2 \times 10^{-4}$	4.8 96
Crowned Idler (Right) (.00016)			12	.75	7.5	4.3	$6 \times 10^{-3}$	$1.6 \times 10^{-4}$	4.8 80
Reels Ripple Torque	Excitation 1.5 in - oz @ Ripple Frequency 46x Speed								

Table 3.9  
Calculated Tape Response at the Head for Five-Year Recorder

Tape Speed (Cause)	Displacement		Velocity
	Amplitude (in)	Frequency (rad/sec)	Flutter Percent
3 ips (Eccentricity)	$1.37 \times 10^{-2}$	4.8	0.15
60 ips (Eccentricity)	$1.37 \times 10^{-2}$	96	0.15
7.5 ips (Ripple Torque)	$0.37 \times 10^{-2}$	115	0.4
60 ips (Ripple Torque)	$0.37 \times 10^{-5}$	920	0.004

In order to determine the jitter from the vibration response data, the relative tape displacement between data is obtained from the following relationship:

$$\text{Jitter} = \sum_{i=1}^n \chi_i(t + \tau) - \chi_i(\tau)$$

where

$\chi_i(t + \tau)$  = tape displacement at time =  $t + \tau$  due to  
ith disturbance

$\tau$  = bit spacing in seconds

$\chi_i(t)$  = instantaneous tape displacement due to  
ith disturbance

For a given disturbance, the tape displacement is harmonic and, therefore

$$\chi_i = a_i \sin(\omega_i t - \phi_i)$$

where

$a_i$  = disturbances amplitude

$\phi_i$  = disturbance phase angle

$\omega_i$  = disturbance frequency

Then the jitter for the ith disturbance is

$$\tau_i = \left[ a_i \sin \omega_i (t + \tau) - \phi_i \right] - a_i \sin \left[ \omega_i t - \phi_i \right]$$

Expanding the transcendental functions and making small angle assumptions the jitter is

$$\tau_i = a_i \omega_i \cos(\omega_i t - \phi_i)$$

with a maximum value of

$$|\tau_i| \max = a_i \omega_i \tau$$

and

$$\omega_i = \frac{V}{r_i} n_i$$

$$\tau = \frac{B}{V}$$

$$B = \text{in/Bit}$$

$$V = \text{tape speed}$$

$$r_i = \text{disturbing component radius}$$

$$n_i = \text{disturbance order of tape speed}$$

then

$$|\tau_i| \max = \frac{a_i n_i}{r_i} B$$

For a conservative answer, the random addition is bounded by:

$$|\tau_i| \max = \sum_{i=1}^n \frac{a_i n_i}{r_i} B$$

Table 3.10 shows values of jitter computed from results of Tables 3.9 for a 500 bit/in spacing at 3 and 60 ips tape speed.

Table 3.10  
COMPUTER VALUES OF JITTER

TAPE SPEED (Cause)	JITTER (Micro inches)
3 ips (Eccent)	0.44
60 ips (Eccent)	0.44
7.5 ips (Ripple)	2.1
60 ips (Ripple)	0.21

The results of Table 3.10 correlate with the analytical predictions of other investigations as well as with published performance ratings of existing satellite recorders. It is obvious from the calculations that the recorder displays a large response at 7.5 ips. This is confirmed by experimental results.

#### 4. TRANSPORT TESTS

In preparation for the transport tests approximately 1600 ft. of 1 inch, 3M Type 900 tape was transferred to the transport. Ends of tape windows, approximately 3/8 by 3/8 inch, were created on the appropriate tape edge approximately 50 ft. from each end of the tape. The tape was then shuttled through 10 complete cycles at 40 ips with 12 oz of tension to stabilize the tape pack. To minimize the effects of gravity, the transport was operated in the vertical plane in all of the tests which follow.

A single reproduce head (Western Magnetics Inc., Model 503800-2, Reproduce, Serial No. 103) was used on record and reproduce in all of the transport tests. This head, which has 4 active channels (No. 1, 3, 21 and 41), was mounted such that channel #1 was closest to the transport deck.

The effects of record and reproduce tension on the reproduced signal level were investigated at tension between 4.5 oz. and 12 oz. and at transport speeds of 3.0 ips record and 60 ips reproduce. Varying the record tension from 4.5 oz to 10 oz produced an average signal level increase of 25%. Above 10 oz no increase in signal level was observed. Varying the reproduce tension between 4.5 oz and 12 oz produced only minor variations in signal level.

##### 4.1 Tracking Accuracy

This series of tests was designed to measure the ability of the transport to move tape across the record/reproduce head in a repeatable manner and to determine the minimum tension required for adequate tape guidance at a record speed of 3 ips and a reproduce speed of 72 ips. Two PhysiTech model 440 auto collimators were positioned to simultaneously measure the displacement of the outside tape edge at the head and at a point near the left reel. The outputs of the PhysiTech units were calibrated to provide a 2.5 mil/mm of pen deflection on a

Sanborn dual channel chart recorder. Due to the geometry of the transport's tape path, front surface mirrors were employed to allow for the viewing of the tape edge in a line perpendicular to the tape travel. Illumination of the target areas was provided by a microscope lamp at the left reel and by a set of four pen light lamps at the head.

In a typical test the transport controls were adjusted to a particular tension/speed combination and a disturbance was introduced into the tape pack near the right end of the tape. The tape was then shuttled through the disturbed portion of tape until the disturbance disappeared. The amount of disturbance attenuation with each cycle of the tape provided a measure of the transport guidance for the particular tension/speed combination under test.

Initial guidance tests at 72 ips and 12 oz of tension indicated that the tape edge had a characteristic short and long term position variation. After 10 complete passes at 72 ips and 12 oz tension, a repeatable tape edge position signature was observed on each successive tape pass. This signature had a short term variation of 3 mils peak-to-peak and a long term drift of 15 mils between the ends of the tape. When a disturbance of approximately 50 mils peak was introduced near the right end of the tape this signature was again observed after 7 complete tape passes through the disturbed area. From this initial test it was obvious that this characteristic tape edge position signature was representative of the tape slitting process and not a function of the transport.

Tests were made at several speed/tension combinations and with and without the tension sensors in place at 3 ips record and 20 ips reproduce. The results of these tests are listed in Table 4.1. An additional long term test was conducted in which

Table 4.1

## SUMMARY OF TAPE TRACKING ACCURACY TESTS

Speed (IPS)	Tension (oz)	Average Attenuation Per Cycle (%)	Average Attenuation of Left Crowned Roller (%)
20	6	30	15
20	12	30	15
72	6	-41	
72	9	18	15
72	12	43	15

Tension-controlled, 3 ips Record, 20 ips Reproduce

3-20                    4                    21

3-20                    6                    31

Torque-controlled,\* 3 ips Record, 20 isp Reproduce

3-20                    4                    55

3-20                    6                    55

---

\* with torque control the tension sensors are no longer part of the tape path.

the controlled tension was changed when the tape changed direction. The tape shuttled for ten passes with a 3 ips/4 oz record and 72 ips/12 oz reproduce combination and a repeatable signature was obtained. The tape was then shuttled for three passes with a 3 ips/6 oz record and 72 ips/12 oz reproduce combination, and three passes with a 3 ips/6 oz record and 60 ips/12 oz reproduce combination, with no degradation of tape guidance.

In another series of tests the level of the reproduced signal was used to measure tape guidance. In these tests the amplified head output was connected to a Hewlett Packard Model 400E voltmeter which has a DC output proportional to rms AC input. The output of the HP 400E was recorded on a Sanborn Chart recorder. The output was measured over the total length of tape in both directions at speeds of 7.5 ips, 30 ips, and 60 ips.

All of the tests were run with 12 oz of tension on record and reproduce. Replaying the tape in the record direction produced short term tracking errors of from 0.5 to 0.7 mils peak-to-peak. In the reproduce direction the short term tracking errors ranged from 0.6 to 0.9 mils peak-to-peak. These results were calculated from the following:

$$\text{p-p tracking error} = \frac{\Delta \text{output}}{\text{min output}} \times \text{effective track width,}$$

where the effective track width is approximately 12 mils.

When the transport reverses direction, the drop in reproduced signal level indicated a steady state tape tracking shift of approximately 1 mil on all of the tests. It is believed that this shift is due to a slight misalignment in the elevation of the crowned rollers. The crowned rollers have provisions for elevation adjustment which can correct this condition.

The results of these tests indicate that adequate tape guidance can be obtained with 12 oz of tension at a reproduce speed of 72 ips and with as little as 4 oz of tension at a record speed of 3 ips. Other tests indicated that the reproduced



signal level was not a strong function of tension but that as record tension increased the reproduced signal increased, leveling off at 10 oz of record tension (see section 4.0).

#### 4.2 Rotational Accuracies

This series of tests was designed to measure the runout of the two capstans and the two crowned rollers. A PhysiTech Model 440 auto collimator was used for these measurements and its output was recorded on a Sanborn chart recorder calibrated to provide .04 mil/mm of pen deflection. A white screen illuminated by a microscope lamp was positioned behind the roller under test and the PhysiTech unit was focused to track the roller's radius as silhouetted against the screen.

The measured data are given in Table 4.2. All of the rollers were measured at the inside and outside tape edge positions. The crowned rollers were also measured at the top of the crown (maximum radius). The relative phase of the capstan runouts was measured by placing a strip of 80 mil wide masking tape on the capstan parallel to the axis of rotation. This tape provides a timing mark once per capstan revolution which was used to determine phase.

Although none of the rollers has a runout greater than 0.6 mil, it was found that the level of dynamic skew of a reproduced signal could be influenced by changing the relative phase of the tension capstan with respect to the tape. The maximum and minimum values of dynamic skew at the capstan rotation rate were in the ratio of 4 to 1. This variation in the skew can be attributed directly to the runout of the tension capstan and to its high coefficient of friction. A similar, but less dramatic, relationship was observed with respect to the speed capstan but it could not be measured because of the strong influence of the tension capstan. No relationship between skew and either crowned roller runout was observed.

Table 4.2  
ROTATIONAL ACCURACY

<u>Roller</u>	<u>Runout (mil p-p)</u>		<u>Center of Crown</u>
	<u>Inside Tape Edge</u>	<u>Outside Tape Edge</u>	
Left Crowned	0.32	0.16	0.20
Right Crowned	0.16	0.36	0.32

<u>Roller</u>	<u>Runout (mils p-p)</u>		<u>Phase</u>
	<u>Inside Tape Edge</u>	<u>Outside Tape Edge</u>	
Tension Capstan	0.60	0.56	63° inside Leads*
Speed Capstan	0.40	0.24	41° inside Leads*

\* Rotating in the record direction.

### 4.3 Flutter and Skew

The purpose of this series of tests was to determine the transport's flutter and skew characteristics and to identify their probable sources. The transport's flutter characteristics were examined both with a Varo Inc. Model FL-4 flutter meter and with a spectrum analyzer which measured the flutter components at the demodulated output of a phase locked loop. The skew characteristics were examined using the phase comparator portion of the phase locked loop.

In a typical test with the Varo flutter meter, a signal was first recorded, at a particular speed/tension combination, on all four active channels connected in series. The 14.5 KHz crystal controlled oscillator of the Varo unit was used as a signal source at a record current sufficient to saturate the tape. The flutter characteristic of each of the channels was then measured on the Varo unit as the tape was replayed in the record direction at the same speed/tension combination as recorded. The dynamic skew of the two edge channels was then measured using the phase comparator portion of a Signetics phase locked loop which provided an output of 4 volts DC for a 180° shift in phase.

The data obtained in the above tests are listed in Table 4.3. All of the tests were made using a record and reproduce tension of 12 oz. The record current at 60 ips and 30 ips record speeds was 15 ma rms and 6 ma rms at 7.5 ips and 3 ips. The reproduced signals were amplified using the combination of a Tektronics Type D differential amplifier and a Hewlett Packard Model 466A amplifier which together provided a gain of 60 db.

The data of Test #3 indicates that 7.5 ips is a particularly bad speed with respect to flutter, and that the majority of this flutter appears in the band between 0.5 Hz and 30 Hz. An analog computer analysis of the transport's natural frequencies predicted that the combination of the left reel and tape pack inertia in conjunction with the compliance of the length

Table 4.3  
FLUTTER AND SKEW

---

Test #1  
60 ips Record and Reproduce

Channel	% RMS Flutter			
	.5-30 Hz	30-300 Hz	300-5 KHz	DC-5 KHz
1	.02	.08	.14	.16
3	.03	.06	.14	.16
21	.03	.05	.12	.13
41	.04	.06	.12	.13

Edge to Edge Dynamic Skew\*                      3  $\mu$  sec peak

---

Test #2  
30 ips Record and Reproduce

Channel	% RMS Flutter			
	.5-30 Hz	30-300 Hz	300-5 KHz	DC-5 KHz
1	.04	.08	.15	.18
3	.03	.07	.13	.16
21	.04	.08	.11	.16
41	.04	.07	.17	.20

Edge to Edge Dynamic Skew\*                      4  $\mu$  sec peak

---

\* measured between channels 1 and 41  
Record Current = 15 ma rms  
Tension            = 12 oz

Table 4.3 (cont.)

FLUTTER AND SKEW

---

Test #3  
7.5 ips Record and Reproduce

Channel	% RMS Flutter			
	.5-30 Hz	30-300 Hz	300-5 KHz	DC-5 KHz
1	1.5	.20	.55	1.6
3	1.3	.16	.60	1.4
21	1.5	.35	2.0	(2.5)**
41	1.0	.20	.90	1.3

Edge to Edge Dynamic Skew\*                      17  $\mu$  sec peak

---

Test #4  
3 ips Record \*\*\* 60 ips Reproduce

Channel	% RMS Flutter			
	.5-30 Hz	30-300 Hz	300-5 KHz	DC-5 KHz
1	.06	.46	.47	.70
3	.04	.45	.47	.70
21	.05	.45	.48	.70
41	.07	.46	.48	.70

Edge to Edge Dynamic Skew\*                      3  $\mu$  sec peak

---

\* measured between channels 1 and 41

\*\* the actual flutter reading was beyond the range of the Varo unit, 2.5% is the rms sum of 1.5, .35, and 2.0

\*\*\* A 725 Hz signal was recorded using a H. P. 205C oscillator as a source.

Record Current = 6 ma rms  
Tension = 12 oz

of tape between the left reel and tension capstan would produce a resonant frequency in the band between 17.6 Hz and 24.9 Hz. Similarly the combination of the right reel and tape pack inertia in conjunction with the compliance of the length of tape between the right reel and the speed capstan would produce a resonance in the band between 13.8 Hz and 19.3 Hz. These natural frequencies are always present, but at 7.5 ips the resonances are excited by torque disturbances generated in the reel motors in the frequency band between 16.3 Hz and 27.4 Hz. The torque disturbances arise from torque ripple in the reel motors at 46 times their rotation rate. At speeds greater than 7.5 ips, the torque disturbances generated by the reel motors are well above the transport's band of natural resonance frequencies while at 3 ips, they are below the band.

The values of edge-to-edge dynamic skew listed in Table 4.3 represent the maximum value of skew observed in each test. As noted in section 4.2, the dynamic skew could be reduced by a factor of four from the value listed by a change of the relative phase of the tape with respect to the tension capstan. At 30 ips a peak dynamic skew of  $4 \mu$  sec represents a peak dynamic tape edge position error of  $120 \mu$  inch. The tension capstan runouts of 0.60 mils pp and 0.56 mils pp represent a tape edge position error of  $260 \mu$  inch peak if we assume  $\frac{.60 + .56}{2} \sin 63^\circ = 520 \mu$  inch pp =  $260 \mu$  inch peak. The difference between those two numbers could be due to tape slippage on the capstan surface and to the fact that the skew was measured at the head and not at the capstan. If we assume that the speed capstan has zero runout and that the head is midway between the capstans, the two numbers are in close agreement.

Additional measurements of the transport's flutter characteristics were made using a Tektronics model 3L5 spectrum analyzer and a Signetics Type NE 562B phase locked loop. The phase locked loop was tuned to have a center frequency of 360 KHz and filtered to provide demodulated outputs in the band from 0 to 15 KHz. A

frequency deviation of 10% from the center frequency was found to induce an output of 1.05 volts DC in the band from 270 kc to 330 kc. Several frequency bands were investigated but all of the significant components of flutter were found to reside in the frequency band between 0 Hz and 1 KHz.

In a typical test a signal was recorded at a speed between 2 ips and 5 ips on all four active channels connected in series. The record frequency was selected such that a 300 KHz signal was obtained at a reproduce speed of 60 ips. Record current in all of the tests was 6 ma rms. The instrumentation was calibrated using a 900 Hz signal at a level of 0.1 volts peak-to-peak as the input to the spectrum analyzer. Gains and sweep speed were adjusted such that the output of the Sanborn recorder, operating at a chart speed of 5 mm/sec, was calibrated to 10 Hz/mm of chart movement with a pen deflection of .04% peak-to-peak flutter/mm with a sweep speed of approximately 21 seconds. Adjusted as described, the instrumentation provided a hard copy record of the flutter spectral data between 0 Hz and 1 KHz with a maximum full scale output of 2% peak-to-peak flutter or .707% rms flutter.

Table 4.4 gives typical results of these tests. Although spectral data were taken throughout the entire tape pass, only the beginning, middle, and end of pass data are listed. All of the data shown were taken with the transport operating in the record direction at 60 ips.

The data of Table 4.4 indicates that the majority of the transport's flutter is generated by the two reel motors. Operating at 60 ips with the left reel nearly full, the left and right reel motors generate ripple torques at approximately 135 Hz and 215 Hz respectively. In the middle of the pass the ripple torques from both motors are at approximately 155 Hz while at the end of the tape pass, where the right reel is nearly full, the left and right reel motors generate ripple torques at approximately 215 Hz and 135 Hz respectively. All of the major components of flutter occur at harmonics of the two ripple torque frequencies.

Table 4.4  
FLUTTER SPECTRUM

Test #1

Recorded @ 3 ips, 15 KHz with torque control

Reproduced @ 60 ips, 300 KHz with torque control.

<u>Beginning of Pass</u>		<u>Middle of Pass</u>		<u>End of Pass</u>	
(Hz)	(%)*	(Hz)	(%)*	(Hz)	(%)*
135	.30	155	.69	135	.22
215	.56	315	.27	200	.71+ **
265	.21	465	.51	270	.11
400	.69	475	.55	400	.71
630	.30			610	.60

Test #2

Recorded @ 3 ips, 15 KHz with torque control

Reproduced @ 60 ips, 300 KHz with tension control.

<u>Beginning of Pass</u>		<u>Middle of Pass</u>		<u>End of Pass</u>	
(Hz)	(%)*	(Hz)	(%)*	(Hz)	(%)*
135	.31	155	.60	135	.19
215	.56	315	.24	205	.71+ **
265	.21	465	.32	265	.11
400	.65	475	.56	400	.69
620	.30			620	.65

\* Percent rms flutter

\*\* Slightly above full scale reading of .71%



Table 4.4 (cont.)

## FLUTTER SPECTRUM

## Test #3

Recorded @ 3 ips, 15 KHz with tension control

Reproduced @ 60 ips, 300 KHz with tension control

<u>Beginning of Pass</u>		<u>Middle of Pass</u>		<u>End of Pass</u>	
(Hz)	(%)*	(Hz)	(%)*	(Hz)	(%)*
135	.34	155	.60	135	.23
210	.43	320	.16	210	.64
270	.06	475	.31	270	.06
400	.52	485	.45	405	.24
650	.05			650	.23

## Test #4

Recorded @ 5 ips, 25 KHz with tension control

Reproduced @ 60 ips, 300 KHz with tension control

<u>Beginning of Pass</u>		<u>Middle of Pass</u>		<u>End of Pass</u>	
(Hz)	(%)*	(Hz)	(%)*	(Hz)	(%)*
135	.48	154	.69	135	.69
210	.43	162	.52	205	.32
265	.12	315	.05	265	.12
400	.10	470	.07	400	.05
630	.04			630	.12

\* Percent rms flutter

Table 4.4 lists only the first three harmonics since they represented the major portion of the flutter's spectral energy. Higher harmonics of both frequencies were observed out to be the 1 KHz spectrum limit but they were much lower in amplitude.

Comparing Test #1 and #2 of Table 4.4 it can be seen that tension control on reproduce has only a minimal effect on flutter. When tension control is in operation on record and reproduce as in Test #3 of Table 4.4 the 2nd and 3rd harmonics of the torque ripple are reduced. Comparing test #3 and #4 indicates that a further reduction in 2nd and 3rd harmonics is obtained when the record speed is increased from 3 ips to 5 ips.

Reducing the record speed from 3 ips to 2 ips increased the flutter amplitude at the harmonics but at the same time reduces the amplitude at the primary frequencies. The flutter remains near a constant level of 0.8% rms as calculated by the rms sum of the major flutter components. The value of 0.8% is in close agreement with the value of 0.7% as measured by the Varo Inc. flutter meter and listed in Test #4 of Table 4.3. Also the frequencies and amplitudes listed for the beginning of the pass in Test #3 of Table 4.4 agree, within the experimental error, with the % flutter for the various frequencies bands as listed in Test #4 of Table 4.3.

#### 4.4 System Resonances

In this series of tests the transport's natural frequencies were investigated. A sinusoidal tension disturbance of 1.2 oz peak was introduced into the tape by exciting the tension capstan's drive amplifiers. Speed variations induced by the tension disturbances were observed by monitoring the filtered tachometer output. Due to tension capstan drive system roll-off, only frequencies up to 500 Hz could be investigated.

In a typical test a sinusoidal signal was introduced into the input of the tension capstan's drive amplifier using a Hewlett Packard Model 204C oscillator as a signal source. The level of tension disturbance was monitored by measuring the AC voltage across a two ohm resistor in series with the tension capstan motor using a HP 400D VTVM. A second HP 400D monitored the AC signal on the filtered tachometer output at a point which develops 100 mv per inch per second.

Table 4.5 lists the results of these tests. All of the measurements listed were made at 6 ips with a 1.2 oz peak tension disturbance. The reduction in the levels of speed variation when the tension is reduced from 12 oz to 6 oz is probably due to reduced friction between the tension capstan and the tape. The increase in the levels of speed variation when the tension control system is disabled is to be expected since the system is designed to remove tension fluctuations up to approximately 300 Hz.

#### 4.5 Conclusions

The transport tests conducted to date indicate that a workable speed/tension combination would be 3 ips/6 oz on record and 60 ips/12 oz on reproduce. This combination of speed and tension would provide adequate tape guidance with low tape and head wear.

The tests indicate that the 12 oz reproduce tension is only needed to assure an acceptable tape pack on the left reel and that adequate signal reproduction can be achieved with 6 oz of reproduce tension. A further reduction in tape and head wear can be accomplished if the tension capstan is used to create a 6 oz tension differential such that on reproduce the tension of the left reel is 12 oz while the tension at the head is 6 oz. This arrangement would have the additional advantages of minimum power consumption and would require a right reel motor only half as large as the left reel motor.

Table 4.5

TRANSPORT NATURAL RESONANCES

SPEED VARIATION PEAKS (ips peak)

	6 oz with tension control	12 oz with tension control	12 oz without tension control
14 Hz*	.035	.042	.050
17 Hz	.10	.14	.23
23 Hz*	.035	.042	.050
110 Hz	.41	.47	.57
175 Hz**	.18	.10	.11
200 Hz	.21	.25	.27
310 Hz*	.035	.042	.050
330 Hz	.14	.16	.16
500 Hz*	.035	.042	.050

---

\* 6 ips system noise level

\*\* Valley in level of speed variation

The flutter test indicates that although the percent RMS flutter is at a reasonable level, a further reduction can be accomplished by the use of better reel motors. Synchronous motors, operated in the slip mode, would produce a much lower ripple torque than the brush type DC motors in the prototype transport.

The skew measurements indicate that the majority of dynamic skew is caused by runout in the tension capstan. To manufacture the capstans with a tighter runout tolerance would seem impractical due to the compliance of their surface. A possible solution would be to assemble more capstan modules than required and then select those with the best runout measurements.

The measurements of natural frequencies give an indication of transport speeds which should be avoided, namely, any speed which will generate component rotation rates at any of the transport's principle mechanical resonances.